Identifying the Isoforms of a Novel Muscle-enriched A-type Lamin-Interacting Protein

Shelley Deeke, B.Sc.(Hons)

Thesis submitted to the Faculty of Graduate and Postdoctoral Studies, in partial fulfillment of the requirements for the M.Sc. degree in Biochemistry

Department of Biochemistry, Microbiology and Immunology
Faculty of Medicine
University of Ottawa

Abstract

A novel gene entitled Muscle-enriched A-type Lamin-Interacting Protein, or MLIP was identified through a yeast-two hybrid screen using Lamin A as bait, in an attempt to shed light on the intricate nature of laminopathies. The objective of this study was to identify MLIP's isoforms. Immunoblotting experiments revealed that MLIP is expressed differentially in both mouse and human tissues. A cloning strategy was performed which demonstrated extensive tissue-dependant alternative splicing, however not all protein bands observed by immunoblotting could be accounted for by the splice variants identified. Hence 5' and 3' Rapid Amplification of Complementary DNA Ends was performed, however only a single 5' and 3' untranslated region was uncovered. MLIP contains five highly conserved regions of homology, one of which contains a consensus SUMOylation site. MLIP was investigated as a substrate for SUMO through *in vitro* and *in vivo* assays, however it was not modified by SUMO. It remains to be determined whether MLIP undergoes other post-translational modification. MLIP's function has yet to be defined; however preliminary experiments in our laboratory and MLIP's association with lamin suggest that it may play a role in tissue differentiation.

Acknowledgements:

I am most grateful to my supervisors Dr. Alexandre F. R. Stewart and Dr. Patrick G. Burgon for welcoming me into their labs and giving me the opportunity to pursue graduate studies. I am eternally thankful for their words of wisdom, guidance and advice. Your everlasting enthusiasm was most helpful throughout the experiments that appeared to be insurmountable. The skills that I have learned during my time at the Heart Institute are beyond price.

I must extend a most grandiose thank you to the members of my thesis advisory committee, Dr. Robin Parks and Dr. Alexandre Blais, for their constructive feedback, suggestions and direction.

To my lab mates past and present, Elmira Ahmady, Lara Kouri, Seham Rabaa, Allen Teng, Branka Vulesevi, Adam Turner, Stanimira Krotneva, Jennifer Kasbary, Nina Gross and Nicholas Tokarew, I am forever in your debt for your morale support, your words of encouragement, and most of all, the shenanigans that helped us get through those impossible days…. Lara your air guitar is legendary. Among all the aforementioned lab mates I must highlight four members, Elmira, Lara, Seham and Branka who rendered my experience in the lab most memorable. Words cannot express my appreciation; I cannot imagine my graduate studies without you.

I must express my gratitude to my neighboring lab members Dr. Adolfo de Bold, Dr. Mercedes de Bold, Linda Connor, Shahreen Amin, Asna Choudhry, Monica Forero, Amy Martinuk and Cassandra Roeske. Thank you for your advice, support and rescuing us when were in dire need of whatever reagent was on backorder.

Lastly I must express my gratitude to my family for all the love, support and encouragement, especially my mom, whom for most of my graduate studies was my carpooling sidekick.

Table of Contents:

List of Abbreviations:

cDNA: Complementary Deoxyribonucleic acid
CMT: Charcot-Marie-Tooth
CPSF: cleavage polyadenylation specificity factor
DCM: Dilated Cardiomyopathy
DMD: Dunchenne Muscular Dystrophy
DMEM: Dulbecco's Modified Eagle's Medium
DNA: deoxyribonucleic acid
EDMD: Emery-Dreifuss Muscular Dystrophy
E. Coli : Escherichia Coli
FBS: Fetal bovine serum
FPLD: Familial partial lipodystrophy-Dunnigan variety
HGPS: Hutchinson-Gilford progeria syndrome
IP: immunoprecipitation
IPTG: Isopropyl β-D-1-thiogalactopyranoside
IRES: internal ribosome entry site
kDa: KiloDalton
LGMD: Limb-girdle muscular dystrophy
LMNA: Lamin A/C gene
LMNB1: Lamin B1 gene
LMNB2: Lamin B2 gene
MLIP: Musle-enriched A-type Lamin-Interacting Protein
NLS: nuclear localization signal
ORF: Open Reading Frame
PAS: poly- adenylation signal
PBS: Phosphate-buffered saline
PCR: Polymerase Chain Reaction
PVDF: Polyvinylidene Fluoride
RACE: rapid amplification of cDNA ends
RNA: ribonucleic acid
RT: Room temperature
SDS-PAGE : Sodium dodecyl sulfate Polyacrylamide gel electrophoresis
Shh : Sonic hedgehog
SUMO: Small ubiquitin-related modifier
TBE: Tris Borate EDTA
TBST: Tris-Base tween-20
TSS: transcription start site
TPO: thrombopoeintin
uORF: upstream Open Reading Frame
UTR: untranslated region

List of Figures

List of Tables

Chapter 1:
Introduction, hypothesis, rationale and objective of proposed study

General Introduction

A-type laminopathies describe an ensemble of diseases that affect a variety of tissues as a result of mutations in the LMNA gene (Worman et al., 2009). The mechanism that links the mutations in the LMNA gene to the disease remains unknown. One of the hypotheses stipulates that mutations in the LMNA gene could result in the loss of interactions between lamins and lamin-interacting proteins (Hübner et al., 2006). In pursuing this hypothesis, a novel protein, entitled MLIP (Muscle-enriched A-type Lamin-Interacting Protein) was identified by Patrick G. Burgon in 2005.

Lamins

Lamin gene family and expression

In mammals, lamins are divided into two classes. The first class, known as A-type lamins includes both lamin A and C, while the second class consists of B-type lamins. Both classes are constituents of the nuclear lamina, which is a network of intermediate filaments. The nuclear lamina itself is an element of the nuclear envelope, which can be found in all somatic cells (Genschel and Schmidt, 2000; Worman et al., 2009).

The LMNA gene in humans contains 12 exons, and alternative splicing at exon 10 allows for the generation of lamin A and C (Machiels et al., 1996). Lamin A and C share the first 566 amino acids, Lamin A has an additional 98 amino acids and Lamin C has an additional 6 amino acids (Machiels et al., 1996).

Lamins B1 and B2 are expressed in most cell types (Stuurman et al., 1998; Wilson, 2000), whereas A-type lamins are expressed in differentiated cells. The absence of Lamin

A/C expression is as a marker of undifferentiated embryonic stem cells (Krohne and Benavente, 1986; Constantinescu et al., 2006).

Lamin structure and maturation process

Nuclear lamins contain a globular amino-terminal end, followed by a central alpha-helical coiled-coil rod domain, and finally a carboxy terminal domain that contains a nuclear localization signal (NLS) (Genschel and Schmidt, 2000; Lin and Worman, 1993). Lamins undergo polymerization, initially forming dimers, which then assemble into polymers, although this process still remains obscure (Worman et al., 2009).

In order to obtain the mature form, lamin A must undergo farnesylation, a post-translational modification that occurs at the cysteine residue in CaaX box (C for cysteine, A for aliphatic amino acid and X for any amino acid) (Clarke, 1992). This modification is however not required for the incorporation of lamin C in the nuclear lamina (Beck et al., 1990). Following farnesylation, Lamin A is cleaved, releasing the aaX amino acids, which then allows for methylation at the farnesylcysteine residue. Lamin A is then subjected to another cleavage, liberating the last 15 amino acids, which also includes the methylated farnesylcysteine (Weber et al., 1989). This final cleavage yields the mature form of lamin A (Sinensky et al., 1994).

Lamins are also subjected to other post-translational modifications, including phosphorylation, which leads to their depolymerization, a process that is necessary for mitosis to occur (Gerace and Blobel, 1980).

Functional Role of Lamin

The nuclear lamina predominantly resides under the inner nuclear membrane. Its leading role is to provide structural support for the nucleus (Aebi, U., et al., 1986). The lamina also plays a role in a variety of cellular processes, such as chromatin organization, transcription and mitosis; therefore the nuclear lamina interacts with DNA, chromatin, transcription factors and proteins from the inner nuclear membrane (Burke, 1990; Dreuillet et al., 2002; Moir et al., 2000).

Lamins and disease

Mutations within the LMNA gene give rise to a variety of diseases, affecting a diversity of tissues, however the mechanism remains unknown. These diseases can be divided into four main categories (Worman et al., 2009). Within the first category are the diseases that cause progeria, also known as premature ageing; in the second category are the diseases that cause peripheral neuropathy; the third category includes diseases that result in partial lipodystrophy; and the forth category comprises the diseases in which striated muscle is affected (Emery, 1989; Eriksson et al., 2003; Genschel and Schmidt, 2000). The phenotypes of these diseases are summarized in **Table 1**.

Table 1: Diseases associated with mutations in A-type lamins.

Disease	Category	Phenotype
Emery-Dreifuss Muscular Dystrophy (EDMD)	Striated Muscle	Skeletal muscle wasting and weakness in addition to cardiomyopathy (Emery 1989)
Dilated Cardiomyopathy (DCM)	Striated Muscle	Enlarged and weakened heart that is unable to pump an adequate amount of blood (Fatkin et al., 1999)
Hutchinson-Gilford progeria syndrome (HGPS)	Progeria	Premature ageing, development of atherosclerosis during childhood, impaired growth, osteoporosis, hair loss and joint abnormalities (Eriksson et al., 2003)
Limb Girdle Muscular Dystrophy (LGMD)	Striated muscle	Affects the voluntary muscles that are found around the pelvic and shoulder area (Genschel and Schmidt, 2000)
Familial partial lipodystrophy-Dunnigan variety (FPLD)	Partial lipodystrophy	Hypertriglyceridemia, insulin resistance, atrophy of the muscles and a decline in subcutaneous fat from the extremities (Garg, 2000)
Charcot-Marie-Tooth disorder type 2B1 (CMT)	Peripheral neuropathy	Lower limbs suffer a loss of deep tendon reflexes as well as weakness and atrophy (De Sandre-Giovannoli et al., 2002)
Atypical Werner Syndrome	Progeria	Aged appearance, cataracts, osteoporosis, vascular disease (Worman et al., 2009)

Mutations in the LMNA gene that give rise to these disorders include nonsense and missense mutations (Emery, 1989), intron retention and in-frame deletion of a codon (Genschel and Schmidt, 2000). A complete lack of A-type lamins in humans results in perinatal lethality, for which there has only been one case reported (Van Engelen et al., 2005). The infant was born pre-maturely and succumbed to the disease promptly after birth due to respiratory failure.

Mutations in LMNA that give rise to muscle-specific diseases are dispersed throughout the LMNA gene as illustrated in **Figure 1**, while nearly 90% of mutations that lead to FPLD2 are found within exon 8, a globular domain (Speckman et al., 2000). It has been reported that DCM and EDMD can both arise from the same mutation within the LMNA gene (Bonne et al., 2000).

Diseases also arise due to abnormalities in the maturation process of lamin A. The depletion of ZMPSTE24, the enzyme responsible for the final cleavage of prelamin A, leads to a perinatal-lethal progeroid syndrome. The loss of this enzyme results in a build-up of farnesylated prelamin A (Navarro et al., 2004).

Figure 1: Laminopathy-linked LMNA mutations.

Exons (top) are coloured according to the lamin protein domains (bottom) that they encode. Lamin A-specific exons are green. Exons that correspond to the 3′ untranslated region are yellow. This figure presents ~50% of the known LMNA disease-linked mutations. CaaX represents a carboxy-terminal farnesylation sequence that is present in lamin A but not lamin C. Reprinted by permission from Macmillan Publishers Ltd: [Nature Reviews Molecular Cell Biology] (Burke, B., Stewart, C.L. Life at the edge: The nuclear envelope and human disease. 8, 575-585), copyright (2002).

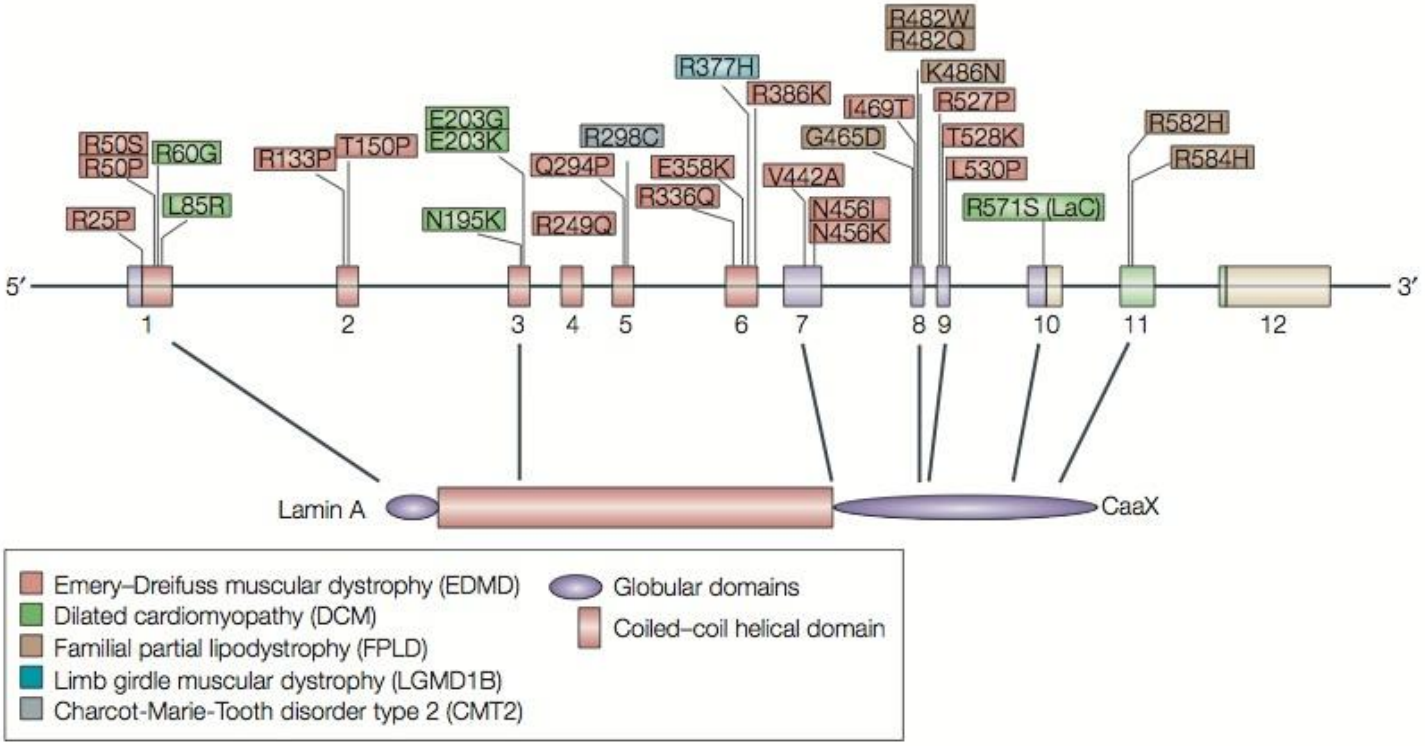
R482W
R482Q
R377H
K486N
R386K
I469T
R527P
E203G
E203K
R298C
G465D
T528K
R582H
R50S
R50P
R60G
R133P
T150P
Q294P
E358K
V442A
L530P
R584H
R336Q
N456I
N456K
R25P
L85R
N195K
R249Q
R571S (LaC)
5′
3′
1
2
3
4
5
6
7
8
9
10
11
12
Lamin A
CaaX
Emery–Dreifuss muscular dystrophy (EDMD)
Dilated cardiomyopathy (DCM)
Familial partial lipodystrophy (FPLD)
Limb girdle muscular dystrophy (LGMD1B)
Charcot-Marie-Tooth disorder type 2 (CMT2)
Globular domains
Coiled–coil helical domain

Breaking new ground: Discovery of MLIP

MLIP or Muscle-enriched A-type Lamin-Interacting Protein (C6orf142) is a novel gene, found exclusively in amniotes. In human, MLIP is located on chromosome 6p12.1 and is 247kilobases (Ahmady et al., 2011)[1]. Our lab discovered MLIP through a yeast-two hybrid screen using the rod 1 domain of human Lamin A/C, amino acids 1 through 230, as bait against a human heart cDNA library. Of the 232 positive interacting clones, 6 were MLIP. Further investigation demonstrated that MLIP interacts between amino acids 1 and 130 of LMNA (Ahmady et al., 2011)[1].

MLIP tissue expression

Northern blotting demonstrated that MLIP is predominantly found in the heart and skeletal muscle in both mouse and human (**Figure 2**). Both species also contain two principal transcripts. In mouse, one was observed at 3.5kbp and the second between 1 to 2 kbp, while in human one was at 3.8kb and the second between 1.35 and 2.4kb (Ahmady et al., 2011)[1].

By means of quantitative PCR on several adult mouse tissues, with the values normalized to that of heart, the highest level of expression was observed in smooth muscle, followed by skeletal muscle, then heart, kidney and finally brain (Ahmady et al., 2011)[1].

[1] Elmira Ahmady, Shelley A. Deeke, Seham Rabaa, Lara Kouri, Laura Kenney, Alexandre F. R.Stewart & Patrick G. Burgon (2011). Identification of a novel Muscle Enriched A-Type Lamin Interacting Protein (MLIP). *Under 2nd revision JBC April 2011*

Figure 2: MLP tissue expression profile

Expression of MLIP mRNA in A) mouse and B) human tissue by Northern analysis revealed two transcripts. 10 µg of poly-A enriched RNA was loaded per lane. C) Normalized tissue distribution of MLIP expression in adult mouse tissue (n=3, mean ± Std.Dev.) as determined by quantitative PCR. Reprinted with permission from authors (Ahmady et al., 2011)[2].

[2] Elmira Ahmady, Shelley A. Deeke, Seham Rabaa, Lara Kouri, Laura Kenney, Alexandre F. R.Stewart & Patrick G. Burgon (2011). Identification of a novel Muscle Enriched A-Type Lamin Interacting Protein (MLIP). *Under 2nd revision JBC April 2011*

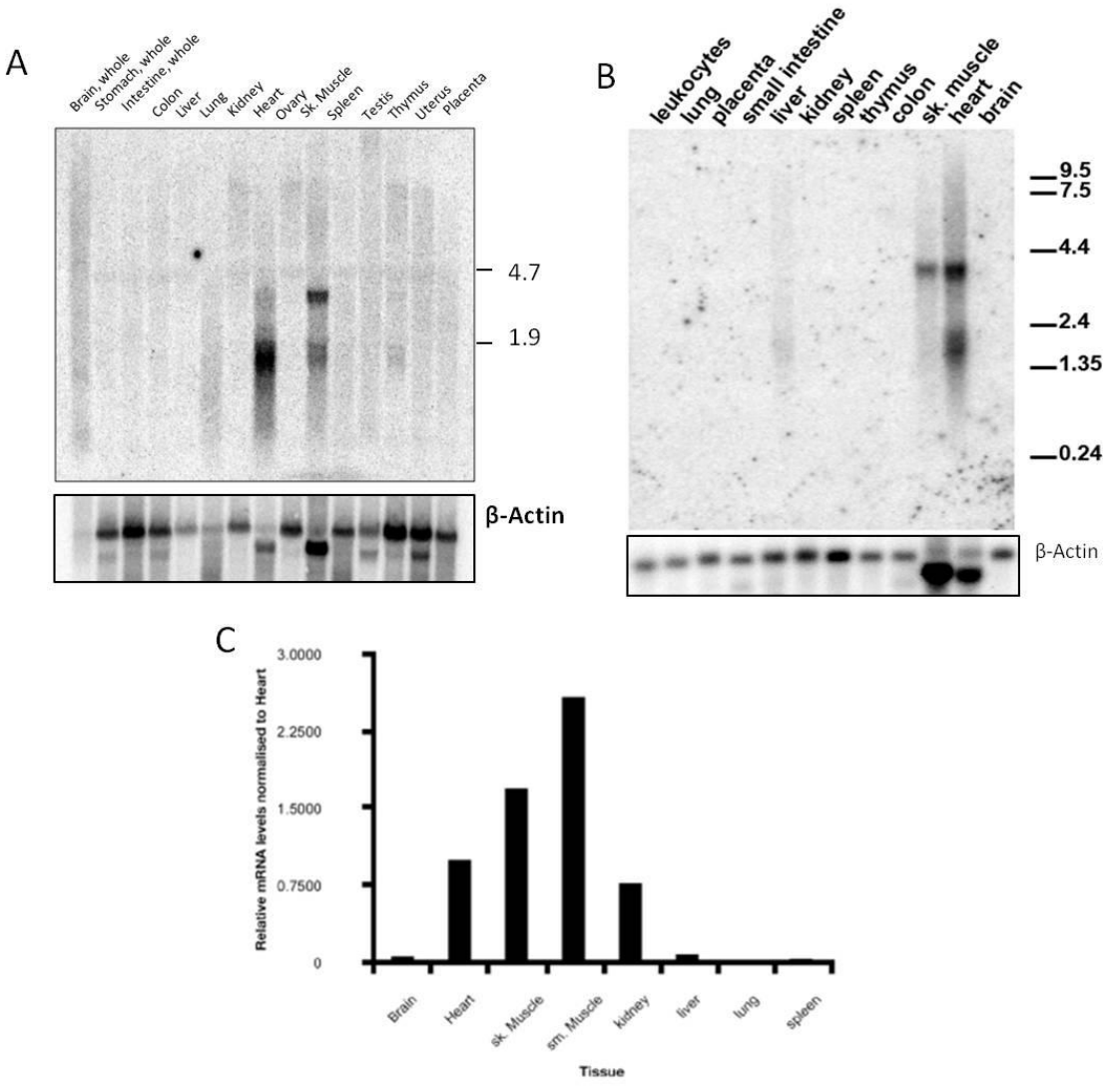
A
Brain, whole
Stomach, whole
Intestine, whole
Colon
Liver
Lung
Kidney
Heart
Ovary
Sk. Muscle
Spleen
Testis
Thymus
Uterus
Placenta
4.7
1.9
β-Actin
B
leukocytes
lung
placenta
small intestine
liver
kidney
spleen
thymus
colon
sk. muscle
heart
brain
9.5
7.5
4.4
2.4
1.35
0.24
β-Actin
C
Relative mRNA levels normalised to Heart
3.0000
2.2500
1.5000
0.7500
0
Brain
Heart
sk. Muscle
sm. Muscle
kidney
liver
lung
spleen
Tissue

Through indirect immunohistochemistry, MLIP has been shown to be present in the mouse brain (hippocampus, cortex, dentate gyrus), skeletal muscle and heart (Ahmady et al., 2011)[1].

MLIP unmatched sequence and subcellular localization

Comparison of the MLIP sequence against the GenBank database did not exhibit any considerable likeness to any other gene (Ahmady et al., 2011)[1]. Thus far, there have not been any homologues of MLIP observed in invertebrates or in anamniotes, which may attribute to the complexity of amniotes (Ahmady et al., 2011)[1]. The alignment of the full-length sequence of MLIP in human, mouse and chicken exhibits five highly conserved regions of homology (**Figure 3**) (Ahmady et al., 2011)[1]. The first highly conserved region of homology, which spans amino acids 123 to 129 contains a putative type I SUMOylation site. The second and third highly conserved regions of homology are of unknown function and span amino acids 380-397 and amino acids 448-467, respectively. The fourth region contains a putative nuclear localization sequence, PENKKSYQ in human, amino acids 721 through 728 and in mouse the NLS sequence consists of PENKKPKQ and spans amino acids 689 to 696. The fifth highly conserved region of homology contains a putative tyrosine-phosphorylation site (Ahmady et al., 2011)[1].

[1] Elmira Ahmady, Shelley A. Deeke, Seham Rabaa, Lara Kouri, Laura Kenney, Alexandre F. R.Stewart & Patrick G. Burgon (2011). Identification of a novel Muscle Enriched A-Type Lamin Interacting Protein (MLIP). *Under 2nd revision JBC April 2011*

Figure 3: Alignment by Clustal W algorithm of MLIP amino acid sequence of human, mouse and chicken.

Yellow lines represent peptide sequences used for the synthesis of the MLIP polyclonal antibodies. The purple line indicates the putative type I SUMOylation site, the green line denotes the putative nuclear localization sequence, while the orange line highlights the putative Tyrosine-phosphorylation site. Asterisks (*****) demonstrate identical amino acids, double points (**:**) represent semi-conservative substitutions, while single points (**.**) denote conserved substitutions. Numbers indicate the position of the last amino acid for each line. Reprinted with permission from authors (Ahmady et al., 2011)[1].

[1] Elmira Ahmady, Shelley A. Deeke, Seham Rabaa, Lara Kouri, Laura Kenney, Alexandre F. R.Stewart & Patrick G. Burgon (2011). Identification of a novel Muscle Enriched A-Type Lamin Interacting Protein (MLIP). *Under 2nd revision JBC April 2001*


hMLIP MELEKREKRSLLNKN--LEEKLTVSAGGSEAKPLIFTFVPTVRRLPTHTQLADTSKFLVKIPEESSDKS-PETVNRSKS-NDYLTLNAGSQQERDQAKLTCPSEVSGTILQEREFEANKL 116
mMLIP MEFGKHEPGSSLKRNKKLEEGVTVSPGDPEAKPLIFTFVPTLRRLPTHIQLADTSKFLVKIPEEPTDKS-PETVNRFEY-SDHMTFSSESKQERVQRILDYPSEVSGRNSQQKEFNTKEP 118
cMLIP MELGKHES----KGRAALEEKQMVTSQESEAKPLTFTFVPSIGQLPTHFEVVDVSKFLVTIPEEPKDLSNQEIINKAKVLSDELSLNSGGQQDRVPAIS---TDSTQTVLQSLVSNSSKG 113
hMLIP QGMQQSDLFKAEYVLIVDSEGEDEAASRKVEQGPPGGIGTAAIRPKSLAISSSLVSDVVRPKTQGTDLKTSSHPEMLHGMAPQQKHGQLTSSPTTSEQLACKPPAFSFVSPTNPNTPPDP 236
mMLIP QGMQKGDLFKAEYVFIVDSDGEDEATCRQGEQGPPGGPGNIATRPKSLAISSSLASDVVRPKVRGADLKTSSHPEIPHGIAPQQKHGLQK-------------------------TPPVP 213
cMLIP E-MQENDLFKAEFILITDSGDEDEAGAASIN----------AQRPS-------------------------------NGPGP---------------------------------- 153
hMLIP VNLEGASVLEEFHTRRLDVGGAVVEESATYFQTTAHSTPFSASKGTSSTLLFPHSTQLSGSNLPSSTAADPKPGLTSEVLKKTTLTSHVLSHGESPRTSSSPPSSSASLKSNSASYIPVR 356
mMLIP ANVSGATVLREFHTRRLDVTGASEEETTTYFHSTAHDSPLSAWKG-ASTLVVSPSAQLSGSSLCGSNVTDHTRGLASEAQKKMS-TSNVLNPKEDVRTCPAP-ASGASLTSPSASYIPVR 330
cMLIP ----------
hMLIP IVTHSLSPSPKPFTSSFHGSSSTICSQMSSSGNLSKSGVKSPVPSRLALLTAILKSNPSHQRPFSPASCPTFSLNSPASSTLTLDQKEKQTPPTPKKSLSSCSLRAGSPDQGELQVSELT 476
mMLIP IVMHSLSPSPKPLTSSSHGSLSTVCSQMSSSGSLSKSGLKSPVPSRLSLLTAILKSNPSHQRPLSPASCPTFSLNSLASSTLALDQKVKQTPPTSKKSLSSGSLTTGSTEQ-EHQASAAS 449
cMLIP ----------ISAQLLATSHVS-PGMES---------- -RKPPSDGHLPSATLSHSTADQ--------- 191
hMLIP QQSFHLPVFTKSTPLSQAPSLSPTKQASSSLASMNVERTPSPTLKSNTMLSLLQTSTSSSVGLPPVPPSSS-LSSLKSKQDGDLRGPENPRNIHTYPSTLASSALSSLSPPINQRATFSS 595
mMLIP YQPCHLPFFSKTTPLSQAQPLSPLALASNSCASMDIEKIPGSTLRSNTTSPQPQTDTFSLADVPSVTPVLSPLSSSKGRKDGDSRTPEKNRNICIQPSTLAS------TPPVDESLALSS 563
cMLIP ----------
hMLIP SEKCFHPSPALSSLINRSKRASSQLS-GQELNPSALPSLPVSSADFASLPNLRSSSLPHANLPTLVPQLSPSALHPHCGSGTLPSRLGKSESTTPNHRSPVSTPSLPISLTRTEELISPC 714
mMLIP SGKGFHPSPALSDLIDRSKRACSQQHPGQRPSPSALPTPPVSRAASASHPHLGCSILPLQSSLTQTLQPSPSALRPSCGSATCPSRTQMPENTASNHSSRVSTPSLPVSLTRTKELFSPC 683
cMLIP ----------
hMLIP ALSMSTGPENKKSKQYKTKSSYKAFAAIPTNTLLLEQKALDEPAKTESVSKDNTLEPPVELYFPAQLRQQTEELCATIDKVLQDSLSMHSSDSPSRSPKTLLGSDTVKTPTTLPRAAGRE 834
mMLIP ALSMSAGPENKKPK-YKTMSSYKAFAAIPTNTLLLEQKALDEPARTESNSKASVLDLPVE----------HSSDSPSRPPQTMLGSETIKTPTTHPRAAGRE 774
cMLIP ----------QNQQQYKIKTSYKAFAAIPTNTLLMEQKALEEPTKAADVTEGSILDTHSEMCSPAQLRQQTEELCAVIDQVLQDPLTMRRCESSPSFLHMNTESDVGKVSTTLQRAAGRE 301
hMLIP TKYANLSSPTSTVSESQLTKPGVIRPVPVKSRILLKKEEEVYEPNPFSKYLEDNSDLFSEQ---------- 895
mMLIP TKYANLSSSSSTASESQLTKPGVIRPVPVKSKLLLRKDEEVYEPNPFSKYLEDNSGLFSEQ---------- 835
cMLIP TRYANLYKSTPVVAESQMTKPGVIRPVLVKGRIAQQK-EELYQPNPFKKYLEEISDQDVEQPSHPIVPIPENETLSSKEVTNERGSV 387

Subcellularly MLIP can be found in both the nucleus and cytosol, and has also been shown to co-localize with lamin A/C within the nuclear envelope and also with PML bodies (**Figure 4**).

Figure 4: MLIP co-localizes with Lamin A/C and PML bodies in mouse C2C12 myoblasts.

A-D) Mouse C2C12 myoblasts were analysed by indirect immunofluorescence microscopy (Carl Zeiss AxioImager Z1 Microscope) with antibodies against MLIP and Lamin A/C. A) DNA was stained with DAPI, B) Lamin A/C and C) MLIP. D) Merged images of DAPI (blue), Lamin A/C (red) and MLIP (green) staining from panels A-C. Arrow indicates nuclear envelope and co-localization of MLIP with Lamin A/C. E-H) C2C12 myoblasts were analysed by indirect immunofluorescence and sequential scanning confocal microscopy with antibodies against MLIP and PML. E) DNA was stained with DAPI, F) PML and G) MLIP. The arrows indicate co-localization of MLIP with PML. H) Merged images of DAPI (blue), PML (red) and MLIP (green) staining from panels E-G. Scale bar = 10μm. Reprinted with permission from authors (Ahmady et al., 2011)[3].

[3] Elmira Ahmady, Shelley A. Deeke, Seham Rabaa, Lara Kouri, Laura Kenney, Alexandre F. R.Stewart & Patrick G. Burgon (2011). Identification of a novel Muscle Enriched A-Type Lamin Interacting Protein (MLIP). *Under 2nd revision JBC April 2011*

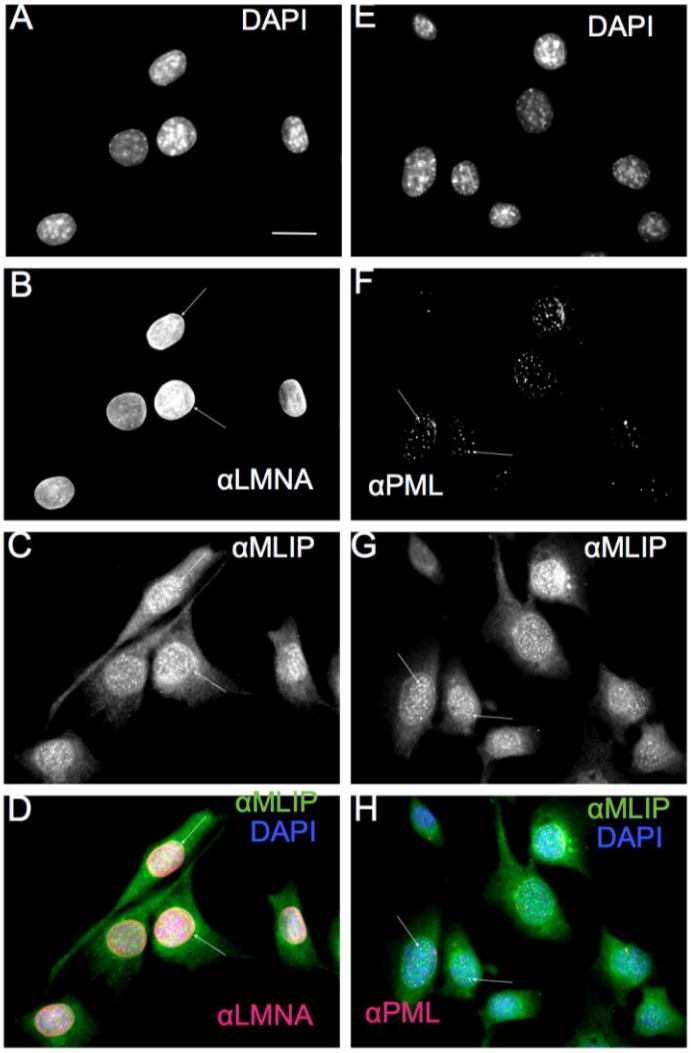
A
DAPI
E
DAPI
B
αLMNA
F
αPML
C
αMLIP
G
αMLIP
D
αMLIP
DAPI
αLMNA
H
αMLIP
DAPI
αPML

Splicing

Preliminary experiments suggested that MLIP may be subjected to alternative splicing. At the 5' splice site of all putative introns, a GU can be found, and at the 3' splice site an AG can be found, which are the splice signals for the major spliceosome (Ahmady et al., 2011)[1].

Splicing is defined as the removal of introns from a precursor mRNA, followed by the ligation of the exons (Black, 2003). Alternative splicing allows for more than one mRNA to be produced from a single pre-mRNA (Chabot, 1996). This process allows the genome to increase its coding capacity (Tazi et al., 2009).

It has been proposed by Wang et al., that alternative splicing occurs in greater than 90% of human genes. Alternative splicing is thought to be an important contributor to the complexity of higher eukaryotes (Kim et al., 2008).

Introns account for more than 90% of the pre-mRNA. The average size of an intron consists of 1000-2000 base pairs, which is approximately 10 times larger than the average exon (Lander et al., 2001). Introns can be present in both coding and untranslated regions (Roy and Irimia, 2009). A mRNA's stability, localization and translational efficiency can be modified based on alternative splicing of the untranslated region (Kim et al., 2008).

[1] Elmira Ahmady, Shelley A. Deeke, Seham Rabaa, Lara Kouri, Laura Kenney, Alexandre F. R.Stewart & Patrick G. Burgon (2011). Identification of a novel Muscle Enriched A-Type Lamin Interacting Protein (MLIP). *Under 2nd revision JBC April 2011*

Splicing Event

The most frequent and simplest splicing in eukaryotes occurs via a two-step reaction. A specific internal adenine mediates the first step (Roy and Irimia, 2009). The 2'-OH of this "branch point" nucleophilically attacks the first nucleotide of the intron. In the second step the last nucleotide of the upstream exon nucleophilically attacks the downstream exon (Roy and Irimia, 2009). These two reactions are catalysed by the spliceosome (Kramer, 1996). The splicesome consists of five small nuclear RNA proteins (snRNPs) U1, U2, U4, U5 and U6. Each one of these snRNPs has their own RNA and interacting proteins (Ritchie et al., 2009). Within the splice site, as well as proximal to the splice site, there are conserved sequences that direct the assembly of the subunits that give rise to the spliceosome (Ritchie et al., 2009). For the stepwise assembly model, it is thought that the splicesome is assembled *de novo* for each splicing event (Rino and Carmo-Fonseca, 2009). U1 snRBNP is the first to bind to the pre-mRNA at the 5' splice site, followed by U2 which associates at the branchpoint and finally U4, U5 and U6 bind to the complex pre-assembled (Rino and Carmo-Fonseca, 2009). Several conformational as well as content changes occur, giving rise to the detachment of U1 and U4 which leads to the activated complex (Rino and Carmo-Fonseca, 2009). Once splicing is complete the subunits of the spliceosome separate and can be reassembled on a different pre-mRNA and execute other splicing events (Rino and Carmo-Fonseca, 2009). Another model proposed is that of the pre-formed spliceosome, or "holospliceosome model" which would allow for a greater splicing efficiency (Azybel et al., 2006). Once the introns have been excised, the pre-mRNA undergoes 5'capping as well as 3'polyadenylation, which allows it to be transported into the cytoplasm (Pistoni et al., 2010).

Main splicing signals

The four principal splice signals are; (1) the 5' splice site which is located upstream of the exon-intron boundary; (2) the 3' splice site which is located downstream of the exon-intron boundary; (3) the branch site; and (4) the polypyrimidine tract which is found between the branch site and the 3' splice site (Kim et al., 2008). These main splice signals have however been estimated to provide only half of the signals necessary for the exon-intron boundary to be recognized by the splicing machinery (Lim and Burge, 2001).

Types of alternative splicing

There are four principal groups of alternative splicing (**Figure 5**). The first group consiste of exon skipping, which is the most common type of alternative splicing in vertebrates and invertebrates accounting for approximately thirty to fourty percent (Kim et al., 2007; Sugnet et al., 2004). The second group is the alternative 5' splice site, also known as the alternative acceptor site, in which there is at least two splice sites at the 5' end of an exon. The third is the alternative 3' splice site, also known as the alternative donor site, in which there is a least two splice sites at the 3'end of the exon. The last type of alternative splicing is intron retention (Kim et al., 2008).

Figure 5: Schematic representation of alternative splicing.

The four main types of alternative splicing are ;1)exon skipping; 2)alternative 5' splice site; 3) 3'alternative splice site; and 4)intron retention. Green and blue lines represent alternative splicing, while the black line represents introns and purple boxes denote exons. Adapted by permission from Macmillan Publishers Ltd: [Nature Reviews Genetics] (Cartegni, L., Chew, S. L., & Krainer, A. R. Listening to silence and understanding nonsense: exonic mutations that affect splicing. 3, 947-956.), copyright (2002).

Exon Skipping

Alternative 5′
splice site

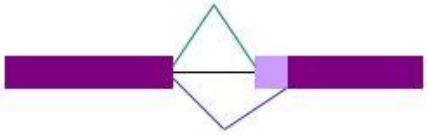

Alternative 3′
Splice site

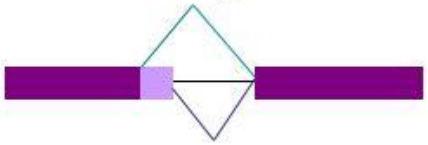

Intron Retention

5' Untranslated Region

It had not yet been established whether MLIP contained a single or alternative 5' untranslated region (UTR). The translation rate of a mRNA is influenced by many characteristics of the 5' untranslated region (UTR). The length, stability, secondary structures, presence of internal ribosome entry sites (IRES), upstream Open Reading Frames (uORF) as well as binding sites for repressor or promoter proteins found within the 5'UTR all affect the translational efficiency (Pickering and Willis, 2004). In humans, 210 nucleotides has been shown to be the average length of the 5' UTR, and the minimum length to be no less than 18 nucleotides (Chatterjee and Pal, 2009). Mutation within the 5'UTR can hinder protein synthesis and lead to various types of disease. For example, hereditary thrombocythaemia is a condition in which there is an overproduction of thrombopoeintin (TPO) which leads to an elevation in platelet counts and can result in abnormal blood clotting or bleeding (Chatterjee and Pal, 2009). This disease can be caused by mutations in the 5' UTR which disrupt one of thrombopoeintin's uORF. In a normal individual, the TPO mRNA contains seven uORFs, which inhibits its translation, uORF7 exhibiting the strongest inhibition on TPO's translation. If uORF7 is shortened, eliminated or frame-shifted to become in-frame with the TPO ORF, the repression is lost and gives rise to the disease (Chatterjee and Pal, 2009).

5' Untranslated Region and protein translation

An important level of control for gene expression occurs at the level of translation for which the 5' untranslated region plays an important role (Gray and Wickens, 1998). Translation initiation occurs through two main mechanisms in eukaryotes. The first

mechanism is by means of cap-dependent initiation and the second through internal ribosome entry (Pickering and Willis, 2004). Cap-dependent initiation involves many eukaryotic initiation factors that assemble to form a pre-initiation complex. This pre-initiation complex then interacts with the 5' cap structure, which renders it able to scan for the initiation codon. The 5' cap is a guanine nucleotide, methylated at the seventh position, that is linked to the 5' end of a mRNA through a 5' to 5' triphosphate linkage (Robins et al., 1976). Once the complex recognizes the initiation codon, the initiation factors are liberated and the 60S ribosomal subunit is recruited giving rise to the 80S ribosome which can begin the elongation step of protein translation (Pickering and Willis, 2004).

The second mechanism of translation initiation involves the internal ribosome entry site (IRES), which is a portion of secondary structure found within the 5'UTR (Pickering and Willis, 2004). Many of the mRNAs that contain IRESs are implicated in processes that regulate cell fate, such as growth, differentiation, proliferation, apoptosis and response to heat shock and hypoxia. Some of the initiation factors required for IRES are also necessary for cap-dependent scanning (Pickering and Willis, 2004). The first IRESs were identified in the poliovirus (Pelletier and Sonenberg, 1988) and the encephalomyocarditis virus (Jang et al., 1988) in 1988, however IRESs have also been shown to be present in cellular mRNAs (Macejak and Sarnow, 1991). It has been possible to predict some IRESs in viruses based on sequence conservation of related viruses, however, cellular IRESs have almost nothing in common when examining parameters such as sequence or secondary structure and therefore cannot be predicted (Mokrejs et al., 2009).

3'UTR

Whether MLIP contains a single or alternative 3'UTR remains to be determined. The stability, localization and translation of mRNA also relies on the 3'UTR. If a mutation alters the secondary structure of the 3'UTR, the polyadenylation signal or the stop codon, translation can be impaired and thus lead to disease. For example, the GATA4 gene in patients that suffer from congenital heart disease was analyzed and some of the mutations uncovered were present within the 3'UTR (Reamon-Buettner et al., 2007). In mammals, the transcription factor GATA4 is essential for cardiac development, playing a role in heart tube formation and ventral morphology, with the complete loss of GATA4 causing lethality (Molkentin et al., 1997). The mutations within the 3'UTR are thought to alter mRNA folding and thus modifying the secondary structure, which could potentially affect translation (Reamon-Buettner et al., 2007). It has been previously shown that modest adjustments in the level of protein expression of GATA4 leads to a striking effect in cardiac development and fatality (Pu et al., 2004).

Polyadenylation

Polyadenylation occurs via a two-step reaction. In the first step the nascent mRNA is subjected to cleavage and in the second step a polyadenine tail is added (Colgan and Manley, 1997). The most common motif of polyadenylation signal (PAS) is AAUAAA (Chatterjee and Pal, 2009). Polyadenylation signals are the binding location for the cleavage polyadenylation specificity factor (CPSF). The PAS hexamer is normally located ten to thirty nucleotides upstream of the cleavage site, however it has been shown that there are eleven variants of this hexamer with a single nucleotide substitution that can also act as polyadenylation signal (Zhang et al., 2005; Beaudoing et al., 2000).

Post-translational modifications

Post translational modification remains an explanation for a differing number of protein bands immunoblottted when compared to the number of splice variants. Post-translational modifications can modify a protein's biochemical properties, binding partners, stability, conformation (Hicke et al., 2005; Wold, 1981), subcellular localization, while also allowing the regulation of a protein's function without affecting its turn-over (Jürgen Dohmen, 2004). There are an assortment of post-translational modifications, some of which are summarized in **Table 2**.

Table 2: Post-translational modifications

Examples of post-translational modifications, along with their molecular weight, modified residue, known substrates and processes associated with.

Post-translational modification	Molecule added	Molecular weight of modification (Daltons)	Modified residue	Known substrates	Processes involved in
Acetylation	Acetyl group (CH_3 CO)	43Da	Lysine	Histones (Gershey et al., 1968)	Chromatin remodeling (Jenuwein and Allis, 2001)
Methylation	Methyl group (CH_3)	15Da	Lysine Arginine (Kakimoto, 1971)	Histones H3 and H4 (Allfrey and Mirsky,1964) p53 (Kachirskaia et al., 2008)	Chromatin remodeling (Flanagan et al., 2005) Stabilization (Kachirskaia et al., 2008) Acceleration of proteolytic degradation (Esteve et al., 2009)
Neddylation	NEDD8	9,000Da	Lysine (Abida et al., 2007)	p53 (Abida et al., 2007)	Inhibits transcription (Abida et al., 2007) Accelerates the formation of the E2-E3 complex, which stimulates protein polyubiquitylation (Kawakami et al., 2001).
Palmitoylation	Fatty acids, such as palmitic acid $CH_3(CH_2)_{14}COOH$ $(_{16})$	Palmitic acid 256Da	Cysteine	CD36/FAT (Thorne et al., 2010)	Protein Stabilization (Thorne et al., 2010)
Sumoylation	SUMO	11,500Da	Lysine	RanGAP1 (Matunis et al.,1996)	Target Proteins to the nucleus (Matunis et al.,1996)
Ubiquitination	Ubiquitin	8,600Da	Lysine	p105 (Palombella et al., 1994)	ATP-dependent proteolysis (Palombella et al., 1994). Stress-related response

					(Bond and Schlesinger, 1985). Cell cycle control (Glotzer et al., 1991).
Phosphorylation	Phosphate group	94Da	Serine, threonine, tyrosine, histidine aspartate (Schulze et al., 2010)	p53 (Ashcroft et al., 1999; Meek, 1994)	Protein stability (Meek, 1994)

SUMOylation

SUMO (small ubiquitin-related modifier) from the SUMO gene (SMT3), is covalently and reversibly attached to specific lysine residues with most of the target proteins found within the nucleus (Johnson, 2004). SUMO was originally identified in *Saccharomyces cerevisae* (Meluh and Koshland, 1995), but is also found in *Caenorhabditis elegans*, *Drosophila melanogaster*, plants and vertebrates (Geiss-Friedlander and Melchior, 2007). SUMO has been shown to play a role in transcription, DNA repair, chromosome segregation and nuclear/cytoplasmic translocation among many other functions (Hay, 2005; Zhang and Sarge, 2008; Geiss-Friedlander and Melchior, 2007; Dou et al., 2010).

In mammals, there are four SUMO isoforms: SUMO1, SUMO2, SUMO3 and SUMO4, the latter being tissue-specifc, found in the kidneys, lymph node and spleen (Ulrich, 2008, Bohren, 2004). SUMO 1, 2 and 3 are ubiquitously expressed. SUMO2 and SUMO3 are 97% identical but are only 50% identical to SUMO1 (Geiss-Friedlander and Melchior, 2007).

Similarities and distinctions between ubiquitin and SUMO

Ubiquitin and SUMO have similar three-dimensional structures (Bayer et al., 1998) despite the fact that only 20% of their amino acid sequence is identical (Geiss-Friedlander and Melchior, 2007). The dispersion of the charges at the surface of ubiquitin and SUMO are very different (Bayer et al., 1998). The enzymes involved in the sumoylation cascade are distinct from those of the ubiquitin cascade (Geiss-Friedlander and Melchior, 2007).

SUMO maturation process

The immature SUMO protein must undergo proteolysis at the C-terminal end to expose the glycine-glycine motif before it can be covalently attached to target proteins (Mahajan et al., 1998). It remains unknown whether the maturation process is constitutive (Geiss-Friedlander and Melchior, 2007). When SUMO is reversibly added to its target protein an isopeptide bond is formed between the glycine residue at the C-terminal end of SUMO and the lysine residue within the SUMO consensus sequence of the target protein (Mahajan et al., 1998).

SUMO enzymatic cascade

The enzymatic cascade which gives rise to sumoylation involves an E1 heterodimer, an E2 conjugating enzyme Ubc9 and finally an E3 ligase (**Figure 6**). The E1 and E2 enzymes are well conserved through yeast to human (Jürgen Dohmen, 2004). The E1 activating enzyme, Aos1-Uba2, and more specifically a cysteine in the active site of Uba2, forms a thioester bond with the C-terminal glycine of SUMO; this is an ATP dependent reaction (Desterro et al., 1997; Johnson, et al., 1997). SUMO is then transferred to the E2 enzyme Ubc9 via a transesterification reaction, which gives rise to a SUMO-Ubc9 thioester

intermediate (Schwarz et al., 1998). This SUMO-specific E2, binds to the following consensus sequence φKXE/D (x can be any amino acid) and (φ is a large hydrophobic residue), (Sampson et al., 2001) and transfers SUMO to the target protein. An isopeptide bond involves the C-terminal glycine of SUMO and the lysine residue of the SUMO substrate (Mahajan et al., 1998). The transfer of SUMO to the target protein is enhanced by an E3 ligase. In order to be classified as a SUMO E3 ligase, three criteria must be fulfilled. Firstly it must be able to bind Ubc9, secondly it must have the capacity to bind SUMO1 and thirdly, as previously mentioned, enhance the transfer of SUMO to the substrate (Johnson and Gupta, 2001; Braschi et al., 2009). The SUMO E3 ligases can have several different substrates, and therefore it is their cellular localization, which determines their interacting substrate (Braschi et al., 2009).

Crystallography has shed light on the interaction that occurs between a SUMO-acceptor site and the conjugating enzyme Ubc9. A complex composed of Ubc9 and the C-terminal domain of RanGAP1 demonstrated that the lysine residue enters the catalytic pocket of Ubc9, which is predominantly hydrophobic, and the large hydrophobic residue as well as the acidic residue interacts with the surface of Ubc9 (Bernier-Villamor, et al., 2002).

Dissimilarities between SUMO-2/3 and SUMO-1

When under stressful conditions, SUMO-2/3 seems to be mostly conjugated to proteins, while under normal conditions, the majority are modified by SUMO-1 (Saitoh and Hinckey, 2000). *In vivo*, the pool of free SUMO-2/3 is more abundant than that of SUMO-1 (Saitoh and Hinckey, 2000).

In general, a single SUMO unit is added to a lysine residue, however sumoylation can also result in polySUMO chains (Tatham et al., 2001). SUMO-2, SUMO-3, and

SUMO-4 contain a consensus site for the addition of another SUMO, and therefore these three isoforms have the ability to form SUMO chains, this site is however not present within SUMO-1 (Tatham et al., 2001). The function of these SUMO chains has yet to be identified (Geiss-Friedlander and Melchior, 2007), although it has been shown that poly-SUMO chains can lead to ubiquitylation and subsequent degradation (Mullen and Brill, 2008).

Figure 6: SUMOylation Cascade.

SUMO is synthesized as a precursor protein that must be cleaved at its C-terminal end before it can be conjugated to its target protein. This cleavage exposes a Glycine-Glycine motif that interacts with a cysteine residue within the active site of Uba2, one of the members of the E1 activating enzyme. This step requires the hydrolysis of an ATP molecule. Through a transesterification reaction SUMO is transferred from the E1 activating enzyme to the E2 conjugated enzyme Ubc9. Ubc9 interacts with the SUMOylation consensus sequence φKXE/D (φ is a large hydrophobic residue and x can be any amino acid) on the target protein. The E3 Ligase enhances the transfer of SUMO onto the target protein. The SENP, sentrin-specific proteases, can cleave SUMO from its target protein, allowing for this post-translational modification to be reversible. Adapted by permission from Macmillan Publishers Ltd: [Nature Reviews | Molecular Cell Biology] (Geiss-Friedlander, R., F. Melchior. Concepts in sumoylation: a decade on. Nat. Rev. Mol. Cell Biol. 8:947-956.), copyright (2007).

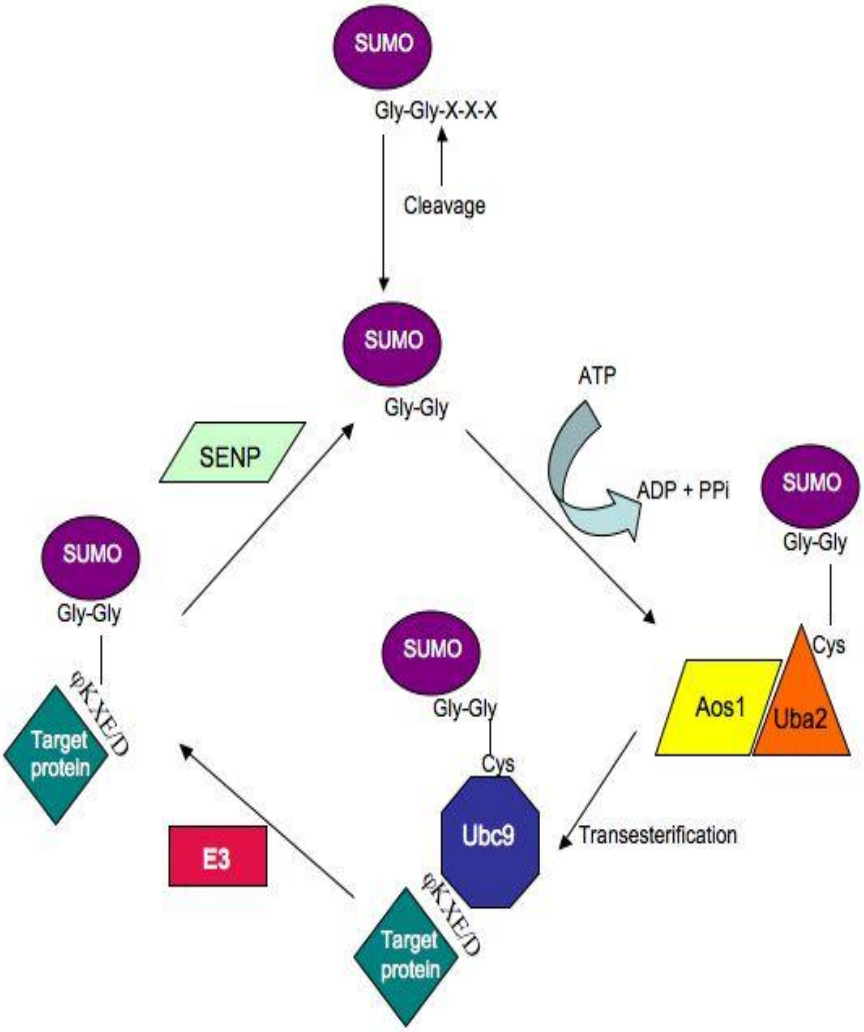
SUMO
Gly-Gly-X-X-X
Cleavage
SUMO
Gly-Gly
ATP
ADP + PPi
SENP
SUMO
Gly-Gly
SUMO
Gly-Gly
Cys
Aos1
Uba2
SUMO
Gly-Gly
Cys
Ubc9
Transesterification
E3
ψK-X-E/D
Target protein
ψK-X-E/D
Target protein

Cell lines

The HL-1 cardiac muscle cell line is derived from cancerous cardiomyocytes of AT-1 mice. This cell line retains the electrophysiological characteristics of cardiomyocytes, the morphology of differentiated cardiomyocytes as well as the capacity to contract (Claycomb et al., 2008). The gene expression profile for HL-1 cells, as assessed by RT-PCR of specific transcripts, seems to be qualitatively similar to adult mouse atrial cardiomyocytes (Claycomb et al., 2008).

The C2C12 mouse myoblast cell line was originally isolated from C3H mice, whose thigh muscle was subjected to injury by crushing, and myoblast cells were cultured 70h after the injury was inflicted (Yaffe and Saxel, 1977). These cells are able to proliferate and differentiate in culture (Yaffe and Saxel, 1977).

Hypothesis, Rationale and Objective of proposed study

An antibody to MLIP had been generated and immunoblotting experiments displayed several different isoforms. My objective was to identify the different MLIP isoforms.

HYPOTHESES:

1) MLIP undergoes tissue-specific splicing.

2) MLIP is post-translationally modified by SUMO.

SPECIFIC AIMS:

1. Identify the MLIP splice variants through cloning and two-dimensional electrophoresis.

2. Search for alternative 5’ and 3’ untranslated regions through means of 5’ and 3’ Rapid Amplification of Complementary DNA ends (RACE).

3. Assess whether MLIP is post-translationally modified by SUMO through generation of a recombinant MLIP protein and subsequent *in vitro* sumoylation assays. Immunoprecipitation of HL-1 cell lysates to determine if endogenous MLIP is SUMOylated *in vivo*.

Chapter 2:
Experimental Procedures

Experimental procedures

Cell Culture

The mouse C2C12 myoblast cell line was obtained from the American Type Culture Collection (ATCC no.CRL-1772) and were cultured at 37°C in an atmosphere of 10% CO_2 in growth medium (GM) which consists of Dulbecco's Modified Eagle's Medium supplemented with 20% fetal bovine serum (FBS) (Fisher Scientific), 1% vol/vol penicillin-streptomycin (Invitrogen) and 2mM L-glutamine (Invitrogen). In order to stimulate myogenesis, cells were grown in differentiation medium (DM), which consists of DMEM complemented with 2% horse serum (Fisher Scientific) and 1% vol/vol penicillin-streptomycin. Cell culture dishes used were all cell culture treated and were purchased from Fisher Scientific. Mouse HL1 cells line was cultured at 37°C in an atmosphere of 5% CO_2, in Claycomb medium supplemented with 10% fetal bovine serum, 1% v/v penicillin-streptomycin and 2mM L-glutamine.

Immunoblotting for MLIP in mouse and human tissues

Male adult mouse brain, heart, lung, liver, kidney and skeletal muscle were harvested from 129SeVe mice. The skeletal muscle included all muscles found in the leg. Tissues were lysed in 50mM Tris-HCl [pH= 8.0], 200mM NaCl, 20mM NaF, 20mM β-glycerolphosphate, 0.5% NP- 40, 0.1mM Na_3Vo_4, 1xProtease inhibitor cocktail (Roche, 1 tablet/10mL), and 1X Phosphatase inhibitor tablet (Roche 1 tablet/10mL) using a glass homogenizer. Lysates were incubated on ice for 20 minutes and then cleared by centrifugation at 10,000xg for 10 minutes at 4°C. Supernatants were collected and protein concentrations were determined using Bio-Rad protein assay dye reagent concentrate kit

(Biorad) and values read using the Thermo Electron Corporation Helios UV-Visible Spectrophotometer. Human tissues were purchased from Clontech Laboratories (7800-1).

Twenty micrograms of protein was resolved on a 12% 1.00mm thick SDS-TrisGlycine polyacrylamide gel at 150V (Biorad Gel Apparatus) and transferred to PVDF membranes (Millipore) for 1 hour at 100V. Transfer buffer was composed of 190mM glycine, 25mM tris base and 20% cold methanol. Following protein transfer, membranes were blocked in 5% fat free milk (Carnation Instant skim milk powder) dissolved in Tris base-Tween-20 (TBS (500mM Tris, 1.5M NaCl), 0.1% Tween-20) for 1 hour. Membranes were then incubated in an MLIP polyclonal antibody 1:20 000 in 5% fat free milk overnight with gentle shaking at 4$_{o}$C. Polyclonal Antibodies to MLIP were raised in rabbit against two synthetic peptides N-MEFGKHEPGSSLKRNKKNL-C, which includes most of exon 1 and N-LRKDEEVYEPNPFSKYL-C, which is a portion of exon10 (21st Century Biochemicals). The antibody used in all immunoblotting is a mix of both antibodies, to ensure that all isoforms can be detected. Membranes were then incubated with Anti-rabbit IgG, HRP-linked Antibody (Cell Signaling #7074) for 1 hour at room temperature with gentle shaking. Immunoblot signals were detected using a SuperSignal West Pico Chemiluminescent Kit (Thermo Scientific) and developed on X-ray film (Thermo Scientific).

Isolation and growth of mouse primary myoblasts

Muscle from neonatal mouse leg was minced in PBS and subsequently incubated in a collagenase/dispase/CaCl2 solution (1.5 U/ml collagenase D, 2.4 U/ml dispase II, 2.5 mM CaCl2) for 1 hour at 37°C. The slurry was then filtered through a 80μm nylon mesh. The cells were centrifuged for 5 min at 350 X g and resuspended in growth media consisting of of Dulbecco's Modified Eagle's Medium supplemented with 20% fetal bovine serum (FBS)

(Fisher Scientific), 1% vol/vol penicillin-streptomycin (Invitrogen) and 2mM L-glutamine (Invitrogen). Cells were preplated on 60mm collagen-coated tissue culture dishes for 15 minutes. The suspension was then moved to a new 60mm collagen-coated tissue culture dish.

Cloning Strategy to identify MLIP splice variants

Total RNA was extracted using Trizol (Invitrogen) as per manufacturer's instructions. 1.0ug of RNA was reverse transcribed using AffinityScript Multiple Temperature Reverse Transcriptase (Stratagene). cDNA was amplified with primers (IDT) designed to the putative 5' and 3' UTR of MLIP. Primer sequences (3'UTR 5'-CAC TTC CAC TCC AGC TTC C-3'; 5'UTR 5'-ACC TCT CTC TCA TTC TTT CAC CAT G-3'). Gene amplification was carried out as follows: 98 °C for 30S, followed by 35 cycles in 3 steps: 98°C for 10s, 55 °C for 10 s, and 72 °C for 90 s and 72 °C for 1 min using Taq DNA polymerase (NEB). PCR products were confirmed by analysis on a 1% agarose gel stained with ethidium bromide. PCR products were inserted into the pCR®II-TOPO®vector according to manufacturer's instructions. Plasmids were transformed using One Shot® TOP10 Chemically Competent *E. coli* (Invitrogen) according to manufacturer's instructions. Plasmids were sequenced using BigDye Terminator v3.1 cycle sequencing kit (Applied Biosystems) and using primers to T7 (TAATACGACTCACTATAGGG) and SP6 (ATTTAGGTGACACTATAG).

Rapid Amplification of 5' Complementary DNA ends (5'RACE)

Isolation of adult mouse heart mRNA was performed by Lara Kouri M.Sc. candidate, using the Qiagen miRNEasy kit, as per manufacturer's instructions. RNA integrity was

assessed by the Agilent 2100 Bioanalyzer. The RNA integrity number for the mRNA used was 9.10. A specific primer to MLIP (final concentration of 2.5uM), either 1)5'-GTC ACT CCC TCC TCT AAG TTC T-3' or 2) 5-CTA GAA GAA ATA GCC AGA GAC-3', was combined with water and 1ug of total RNA from adult mouse heart , and subsequently incubated at 65°C for 10 minutes. Following the incubation, dNTPs (final concentration of 1mM each), 1X Transcriptor RT reaction buffer, and 10 units of Transcriptor Reverse Transcriptase (Roche 03531317001) was added to the reaction mix and incubated for 30 minutes at 55°C, followed by 5 minutes at 85°C to heat inactivate the Reverse Transcriptase. The cDNA was then purified using the NucleoSpin Extract II Kit (Macherey-Nagel #740609.10). Poly(A)tailing of cDNA was carried out as followed; cDNA, 10X Terminal Transferase Buffer and dATP (final concentration of 0.2mM) was incubated at 94°C for 3 minutes. Following incubation, 20 units of Terminal Transferase (NEB #M0315S) was added to the reaction mix and incubated at 37°C for 20 minutes followed by a 10 minute incubation at 70°C to heat inactivate the Terminal Transferase. PCR amplification of dA-tailed cDNA was completed as followed; the dA-tailed cDNA was combined with 10X Thermo Pol Buffer, dNTPs (final concentration of 0.2mM each), a specific primer to MLIP, either 1)5'-TCT TGT TCC TCT TTA GTG AGC-3' or 2)5'-TCA CCT TGT CTG CAT GTA GCT-3', an oligo dT-anchor primer 5'-GAC CAC GCG TAT CGA TGT CGA CT(16)-3' and 2.5 units of *Taq* DNA Polymerase (NEB#M0267L). Cycling parameters were as follows 94°C for 2 minutes, 10 cycles in 3 steps 1)94°C for 15s 2)54°C for 30s 3)72°C for 40s, 25 cycles in 3 steps 1)94°C for 15s 2)54°C for 30s 3)72°C for 40s, in this last step each successive cycle is elongated by an additional 20 seconds. For the nested PCR, the PCR product was combined with 10X Thermo Pol Buffer, dNTPs (final concentration of

0.2mM each), a specific primer to MLIP, either 1)5'-AGC TTC CTG GTT CAT GCT TTC-3' or 2)5'-TCA CCT TTC TGC ATT CCT TGA-3', an anchor primer 5'-GAC CAC GCG TAT CGA TGT CGA C and 2.5 units of *Taq* DNA Polymerase (NEB#M0267L). PCR cycling parameters are the same as mentioned above. PCR products were TA-cloned, transformed and sequenced as described above.

Rapid Amplification of 3' Complementary DNA ends (3'RACE)

Isolation of adult mouse heart mRNA was performed by Lara Kouri M.Sc. candidate, using the Qiagen miRNEasy kit, as per manufacturer's instructions. RNA integrity was assessed by the Agilent 2100 Bioanalyzer. The RNA integrity number for the mRNA used was 9.10. One microgram of adult mouse heart RNA was DNase treated with 1 unit of RQ1 RNase-Free DNase (Promega #M610A) in 1X RQ1 DNase Reaction Buffer (Promega M198A) for 30 minutes at 37°C, then 1uL of Stop Solution (Promega #M199A) was added and incubated for 10 minutes at 65°C. For First Strand Synthesis 1ug of DNase treated RNA was incubated with an oligo dT-anchor primer 5'-GAC CAC GCG TAT CGA TGT CGA CT(16)-3', 20 units of Protector RNase Inhibitor (Roche #03335399001), dNTPs (final concentration of 1mM each) and 10 units of Transcriptor Reverse Transcriptase (Roche 03531295001) for 1 hour at 55°C followed by a 5 minute incubation at 85°C. In order to amplify cDNA, 1ul of cDNA product was incubated with 10X Thermo Pol Buffer, dNTPs (final concentration of 0.2mM each), a specific primer to MLIP, either 1)5'-TTC ATC ATC CTC AAC AGC GT-3' 2)5'-CCA GGA AGC TCA CTA AAG AGG-3' 3)5'-ACA TGC AGA CAA GGT GAA CAA GGC, an anchor primer 5'-GAC CAC GCG TAT CGA TGT CGA C and 2.5 units of *Taq* DNA Polymerase (NEB#M0267L). Cycling

parameters were as followed 94°C for 1 minute, 35 cycles in 3 steps 1)94°C for 30s 2)56°C for 30s 3)72°C for 2 minutes. PCR products were TA-cloned, transformed and sequenced as described above.

Two-dimensional electrophoresis

Sample preparation

C2C12 myoblasts or C2C12 myotubes were lysed in 7M urea, 2M thiourea, 0.5% CHAPS, 10mM DTT, 0.5% ampholyte pH range (~3.5–9.5) (BIO RAD Cat# 163-112), 1X Phosphatase Inhibitor cocktail (Roche), 1X Protease Inhibitor cocktail (Roche). Cells were scraped from dishes and lysates pipetted into 1.5mL centrifuge tubes. Lysates were incubated on ice for 10 minutes then cleared by centrifugation at 16 000rcf for 30 minutes at 4°C. Supernatants were collected and protein concentrations were determined using Bio-Rad protein assay dye reagent concentrate (BIORAD #500-0006) and values read using the Thermo Electron Corporation Helios UV-Visible Spectrophotometer.

IPG strip rehydration

The IPG strip (ReadyStrip IPG GE Healthcare #163-2000 7 cm, pH 3–10, immobilized pH gradient) was rehydrated using the passive in-gel rehydration with sample method. The IPG strip was rehydrated overnight in a total volume of 125µl, with 13ug of total protein from C2C12 cell lysates. The IPG strip was overlayed with mineral oil, and rehydration was carried out using the Immobiline DryStrip Reswelling Tray (GE Healthcare).

Isoelectric Focusing

Isoelectric focusing was performed as per manufacturer's instructions (GE Healthcare). IPG strips were transferred to the Manifold of the Ettan IPGphor3, immersed in Mineral oil. The Isoelectric focusing parameters were as followed: 1)Step voltage mode, 300 volts for 30 minutes 2) Gradient voltage mode,1000 volts 30 minutes 3)Gradient voltage mode, 5000 volts1h20 4) Step voltage mode 5000 volts 25 minutes.

Equilibration of IPG strips

Strips were equilibrated for 15 minutes in 3mL of reducing equilibration buffer consisting of 6M urea, 2% SDS, 20% Glycerol, 0.375M Tris pH8.8 with 0.1M DTT added fresh. Reducing Buffer was poured off, and 3mL of alkylation equilibration buffer was added for 15 minutes, 6M urea, 2% SDS, 20% Glycerol, 0.375 Tris pH8.8 with Iodoacetamide added fresh.

SDS-PAGE and Immunoblotting

Proteins were resolved on a 12% 1.00mm thick SDS-TrisGlycine polyacrylamide gel at 150V (Biorad Gel Apparatus) and transferred to PVDF membranes (Millipore) as described above

Generating rMLIP

Expression of His-tag rMLIP and mock control

MLIP cDNA was subcloned into a His-tag fusion vector pET100D (Invitrogen) and transformed into the bacterial strain BL21 DE3. During the exponential growth phase, isopropyl-1-thio-D-galactopyranoside (IPTG) was added for a final concentration of 1mM

and the culture was incubated for 3 hours at 37°C with shaking (250rmp), followed by a 10 minute 3000g centrifugation at 4°C. The pellet was stored at -80°C.

Bacterial cell lysis

Bacteria cells were lysed in (20mM sodium phosphate, 500mM NaCl, 20nM Imidazole, pH7.4), 5nM $MgCl_2$, 0.2mg/mL Lysozyme (Sigma #L-6876), 10 units of RQ1 RNase-Free DNase and 1xProtease inhibitor cocktail (Roche, 1 tablet/10.0mL). The solution was stirred for 30 minutes at 4°C, followed by 5 freeze thaw cycles using liquid nitrogen. The solution was then centrifuged at 12000g for 30 minutes at 4°C and the pellet was discarded.

Purification of His-tag rMLIP and mock control

The His-tag recombinant MLIP was purified using a 1mL HisTrap FF column (Amercham Biosciences #1100458) as per manufacturer's instructions. The column was washed out with 5mL of distilled water and subsequently equilibrated with 5 mL of equilibration buffer (20 mM sodium phosphate, 500 mM NaCl, 20mM imidazole, pH 7.4) using a flow rate of 1mL/min. The sample containing the His-tag rMLIP was applied to the column by means of a syringe with a flow rate of 0.2mL/min. The column was washed with 10mL of binding buffer using a flow rate of 1mL/min. Elution was performed through a gradient of imidazole concentration; 2mLs of elution buffer (20 mM sodium phosphate, 0.5 M NaCl, pH 7.4) containing a 50mM concentration of imidazole, followed by 2mL of elution buffer containing 100mM imidazole, 4mLs of elution buffer containing 250mM imidzole and finally 2mLs elution of elution buffer containing 500mM imidazole, using a flow rate of 1mL/min. Elution sample 8, 9 and 10 were pooled and concentrated with an

Amicon Ultra Centrifugal Filter (Millipore #UFC801008). The pooled sample was applied to the filter and centrifuged for 7 minutes for 3000g at 4°C. The sample was then washed with 3mL of PBS.

SDS-PAGE, Coomassie Staining and Immunoblotting of rMLIP and mock control

Proteins were resolved on a 4–15% precast polyacrylamide gel (BIORAD #456-1083) at 200V (Biorad Gel Apparatus). The gel was either subjected to Coomassie staining (0.2% Coomassie Blue, 7.5% Acetic acid, 50% Ethanol) for 1h at room temperature followed by an overnight destaining (50% Methanol, 10% Acetic acid), or proteins were transferred to a PVDF membranes, blocked and probed as described above.

In vitro SUMOylation

In vitro SUMOylation of rMLIP was performed using a SUMOylation kit purchased from Enzo Life Sciences (#BML-UW8955). 200nM of rMLIP or the mock control was incubated for 60 minutes at 30°C in 1X SUMOylation buffer, the SUMO Activating Enzyme Solution (SUMO E1), SUMO Conjugating Enzyme Solution (SUMO E2), SUMO1 or SUMO2 and in the presence or absence of Mg-ATP Solution. The reaction was quenched by adding 2x SDS-PAGE Gel Loading Buffer.

Immunoblotting of In vitro SUMOylation

Ten microliters of the quench reaction was resolved on a 4–15% precast polyacrylamide gel (BIORAD #456-1083) at 200V (Biorad Gel Apparatus). Proteins were transferred to a PVDF membrane (Millipore) for 1h at 100 volts. Transfer buffer contained

190mM glycine, 25mM tris base and 20% cold methanol. Blots that were incubated with SUMO antibodies were blocked overnight in 1%BSA-PBS-Tween (PBS (0.2M phosphate, 1.5M NaCl), 0.1% Tween-20). Membranes were incubated with either anti-SUMO1 (Enzo Life Sciences # PW9460) or anti-SUMO2/3 (Enzo Life Sciences #PW9465)1:1000 in 1%BSA/PBS-T for 1 hour at room temperature. Membranes were washed 3 times for 10 minutes each with PBS/T, then incubated with en Anti-rabbit IgG, HRP-linked antibody (Cell Signaling #7074) 1:2000 in 5% fat free milk for 1 hour at room temperature. Membranes were washed 6 times for 10 minutes each with PBS/T. Blots incubated with the MLIP antibody were manipulated as described above.

Immunoprecipitation

HL-1 cells were lysed in 10mM HEPES (pH 7.4), 50mM NaCl, 0.5mM EDTA, 2mM $MgCl_2$, protease inhibitor cocktail (Roche) and 20mM N-ethylmaleimide added fresh. Cell lysates were incubated on ice for 20 minutes then cleared by centrifugation at 10,000rpm at 4°C for 10 minutes and the supernatant transferred to a fresh tube. Fifty micro liters (1.5 mg) of resuspended Dynabeads® Protein G (Invitrogen # 10003D) was used to bind 5ul of the MLIP antibody or 5ul of the Pre-Immune serum (negative control) in 200 µl PBS -Tween 20 and incubated for 10 minutes at room temperature. The beads-Ab complex was then washed in 200 µl PBS-Tween 20, using magnet for separation. One hundred micro-grams of HL-1 cell lysates was added to the Dynabeads®-Ab complex and incubated with rotation for 1 hour at room temperature. The Dynabeads®-Ab-Ag complex was washed three times using 200 µl PBS for each wash, using the magnet for separation. The Dynabeads®-Ab-Ag complex was resuspended in 100 µl PBS and transferred to a clean tube to avoid co-elution of proteins bound to the tube wall. Supernatant was removed by

means of the magnet and beads were boiled for 10 minutes at 70°C in 1X SDS-PAGE loading buffer. SDS-PAGE and immunoblotting was performed as described above.

Chapter 3:
Results

Results

MLIP protein expression profiles differ between tissues

Male adult mouse brain, heart, lung, liver, kidney and skeletal muscle from WT 129SeVe mice were immunoblotted for MLIP (**Figure 7**). The polyclonal antibody was raised against two synthetic peptides, one recognizes a portion of exon 1 and the second recognizes a portion of exon 10. MLIP is present in all tissues analyzed and its pattern of expression is tissue-dependent. In mouse brain, MLIP has 3 major isoforms, their molecular weights were estimated at 45.1kDa, 42.0kDa and 25.0kDa. In mouse lung MLIP has 3 major isoforms, their molecular weight were estimated at 45.1kDa, 42.0kDa and 26.2kDa. In mouse heart, MLIP has 5 major isoforms, with estimated molecular weights of 42.7kDa, 40.1kDa, 35.8kDa, 34.1kDa, 32.5kDa and 29.5kDa. In mouse liver and kidney, there was a single MLIP isoform with an estimated molecular weight of 42.0kDa. In mouse skeletal muscle there are 2 major isoforms with estimated molecular weights of 40.7kDa and 34.1kDa. **Table 3** contains a summary of the major protein bands along with their estimated molecular weight.

Human testis, pancreas, heart, brain and skeletal muscle were also probed for MLIP **(Figure 7**). In human testis, there are 3 major MLIP isoforms with estimated molecular weight of 45.9kDa, 33.8kDa and 29.9kDa. In human heart, there are 2 major MLIP isoforms with estimated molecular weights of 47.2kDa and 29.9kDa. In human skeletal muscle there are 2 major MLIP isoforms with estimated molecular weights of 75.4kDa and 49.1kDa. MLIP was found to be absent from human pancreas and brain.

Figure 7: MLIP expression pattern differs between tissues

A)Twenty micrograms of protein of male adult mouse brain, lung, heart, liver, kidney and skeletal muscle tissues and **B)** human skeletal muscle, brain, heart, pancreas and testes were probed with a polyclonal antibody to MLIP that was raised against two synthetic peptides. One recognizes a portion of exon 1 and the second recognizes a portion of exon 10. Numbers are in kiloDaltons. Molecular weights of major MLIP protein bands are calculated in **Table 3**.

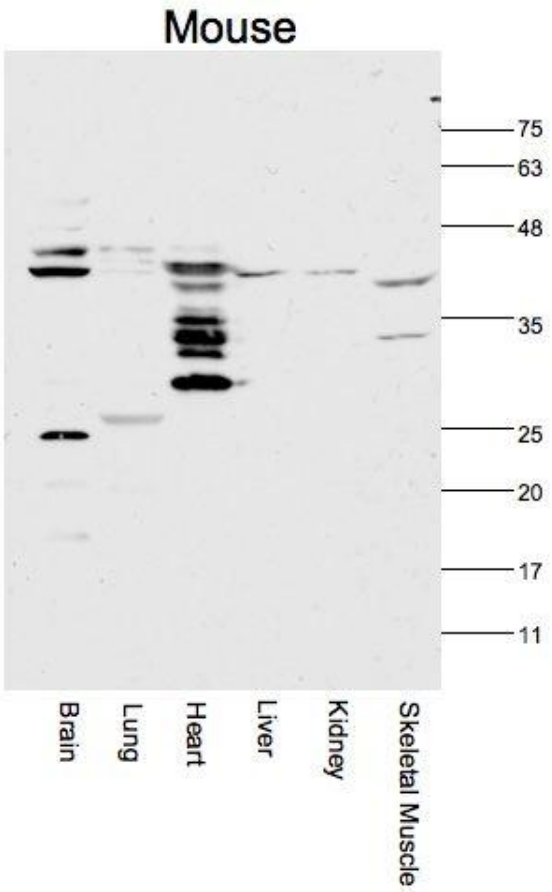
Mouse
75
63
48
35
25
20
17
11
Brain
Lung
Heart
Liver
Kidney
Skeletal Muscle

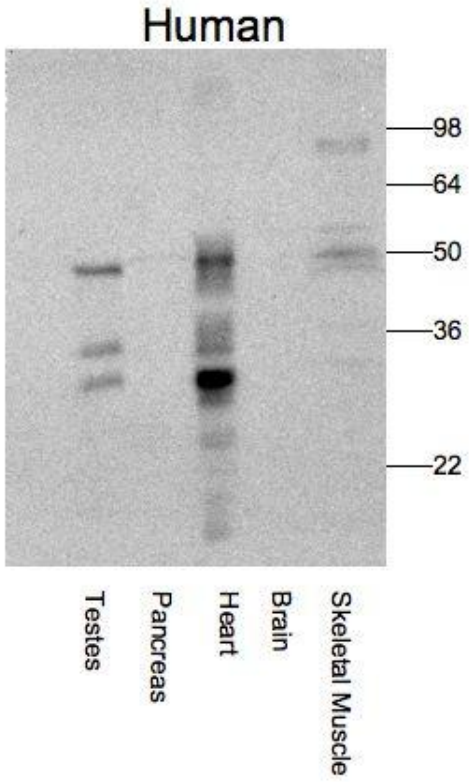
Human
98
64
50
36
22
Testes
Pancreas
Heart
Brain
Skeletal Muscle

Table 3: **Estimated molecular weight of MLIP protein bands in mouse and human tissues.**

Mouse Tissue	Estimated Molecular Weight of Major protein bands
Brain	45.1kDa
	42.0kDa
	25.0kDa
Lung	45.1kDa
	42.0kDa
	26.2kDa
Heart	42.7kDa
	40.1kDa
	35.8kDa
	34.1kDa
	32.5kDa
	29.5kDa
Liver	42.0kDa
Kidney	42.0kDa
Skeletal Muscle	40.7kDa
	34.1kDa

Human Tissue	Estimated Molecular Weight of Major protein bands
Testis	45.9kDa
	33.8kDa
	29.9kDa
Heart	47.2kDa
	29.9kDa
Skeletal Muscle	75.4kDa
	49.1kDa

MLIP is subjected to alternative splicing

The immunoblotting of MLIP in different mouse tissues displays several isoforms. In order to account for the bands observed, a cloning strategy using primers to the putative 5' and 3' untranslated regions was performed to identify possible MLIP splice variants. Previous experiments suggested a functional role of MLIP in myogenesis. These preliminary results demonstrated that knocking down MLIP may have an inhibitory effect on myogenesis and that MLIP may be required for proper myotube formation (Ahmady, M.Sc. thesis). Due to these findings, different sources of striated muscle were analyzed in the cloning strategy. The putative full-length MLIP protein contains 13 exons as illustrated in **Figure 8**. Four splice variants, were identified in the HL-1 cardiac muscle cell line, whereas undifferentiated C2C12 mouse myoblast cells as well as C2C12 myotubes contained the same, single splice variant. Myoblast isolated from a rodent's hindlimb also contained a single MLIP splice variant, however there was a different MLIP splice variant identified in the rodent's hindlimb myotubes. The myoblast from the rodent's hindlimb as well as the C2C12 myoblasts were stimulated to undergo myogenesis by withdrawing serum.

Exons 1, 8, 9 and 10 are ubiquitously expressed in all splice variants identified whereas exons 2, 3 and 6 appear to be cell-type restricted. Exons 4, 5, 7 and 11 were not identified in the cells analyzed. The splice variant containing exons 1, 3, 8, 9 and 10 was identified in all cell lines and tissues analyzed.

Figure 8: MLIP alternative splicing is tissue-specific.

Schematic list of MLIP splice variants identified in different tissues and cell lines, by means of cloning. The putative full-length MLIP protein contains 13 exons. Green boxes indicate exons, numbers above denote exon number, numbers in parentheses below designate the number of amino acids within the exon. Below each splice variant is its theoretical isoelectric point and molecular weight (MW).

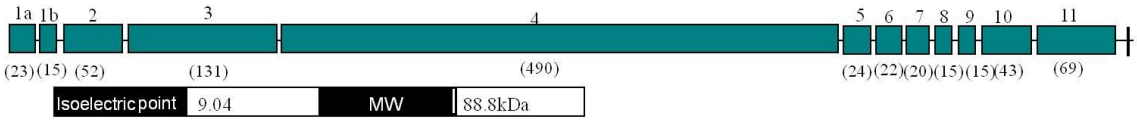

HL-1 cells

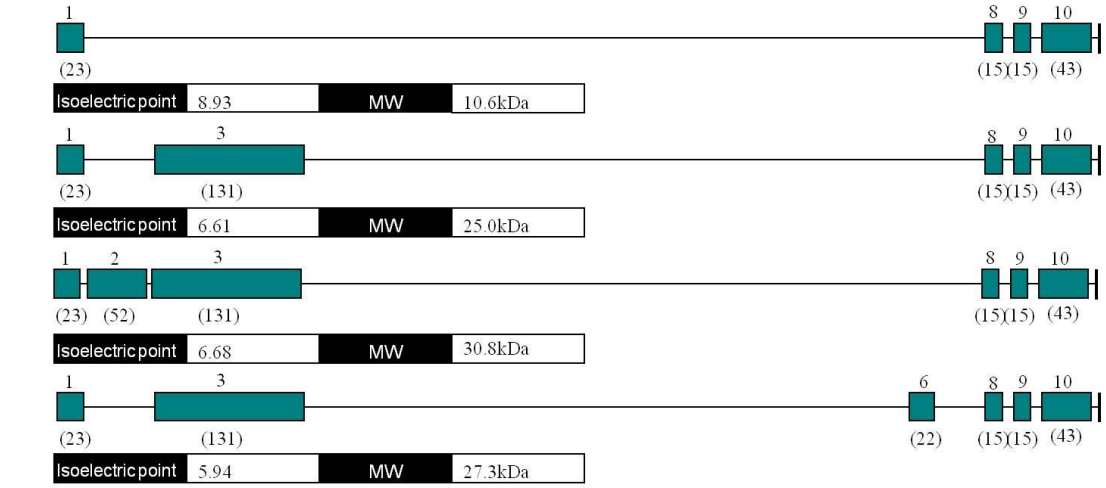

Undifferentiated C2C12

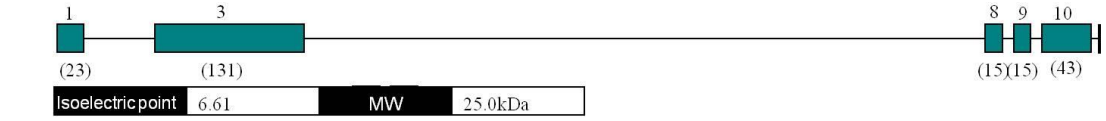

Differentiated C2C12

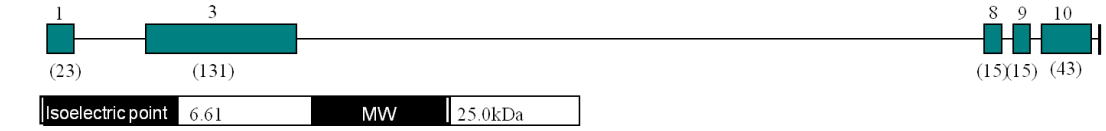

Myoblast isolated from a rodents' hindlimb

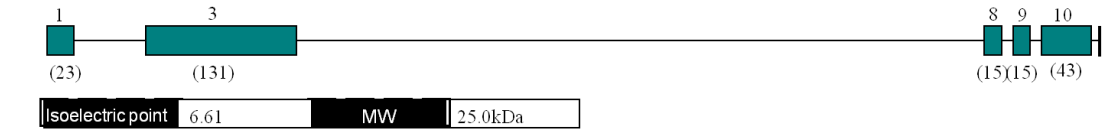

Differentiated myotube from a rodents' hindlimb

Myogenesis of C2C12 cells stimulates the expression of an additional MLIP isoform

C2C12 myoblasts and myotubes were subjected to two-dimensional electrophoresis (**Figure 9**). In order to promote the differentiation of C2C12 myoblasts into myotubes, the media was supplemented with 2% horse serum for 72h in substitution of 10% fetal bovine serum. Two-dimensional electrophoresis separates proteins according to two properties. During the first dimension proteins are separated according to their isoelectric point, which is the specific pH at which the net charge of the protein is zero. In the second dimension proteins are separated according to their molecular weight. As illustrated in **Figure 9**, C2C12 myotubes acquire an additional MLIP isoform as compared to C2C12 myoblast. The MLIP proteins experimental isoelectric point as well as molecular weight were estimated and are found in the table in **Figure 9**.

Comparing the MLIP splice variants that were identified through cloning to the MLIP two-dimensional blots, it is clear that a discrepancy exists. Through cloning only a single splice variant, containing exons 1, 3, 8, 9 and 10, was identified in both C2C12 myoblast as well as in C2C12 myotubes. The theoretical molecular weight of this splice variant is 25kDA and its theoretical isoelectric point is 6.61. This splice variant is in accordance with the spots B and E from the MLIP two-dimensional blots (**Figure 9**). C2C12 myoblasts contain an additional protein spot and C2C12 myotubes contain two additional protein spots unaccounted for by the cloning strategy. The splice variants identified in HL-1 cells also cannot account for the number of protein bands observed by Immunoblotting for MLIP (**Figure 10**). Two possibilities could explain this discrepancy.

The first possibility would be that of alternative 5’ or 3’ untranslated regions and the latter possibility would be that of post-translational modification.

Figure 9: The differentiation of C2C12 myoblasts to myotubes induces the expression of an additional MLIP isoform.

C2C12 myoblast cells were stimulated to undergo myogenesis by removing serum. C2C12 myoblast lysates (top) or C2C12 myotube lysates (bottom) were subjected to two-dimensional electrophoresis. In the first dimension proteins are separated according to their isoelectric point (horizontal axis), and in the second dimension proteins are separated according to their molecular weight (vertical axis). The experimental isoelectric point as well as the experimental molecular weight was calculated (table below).

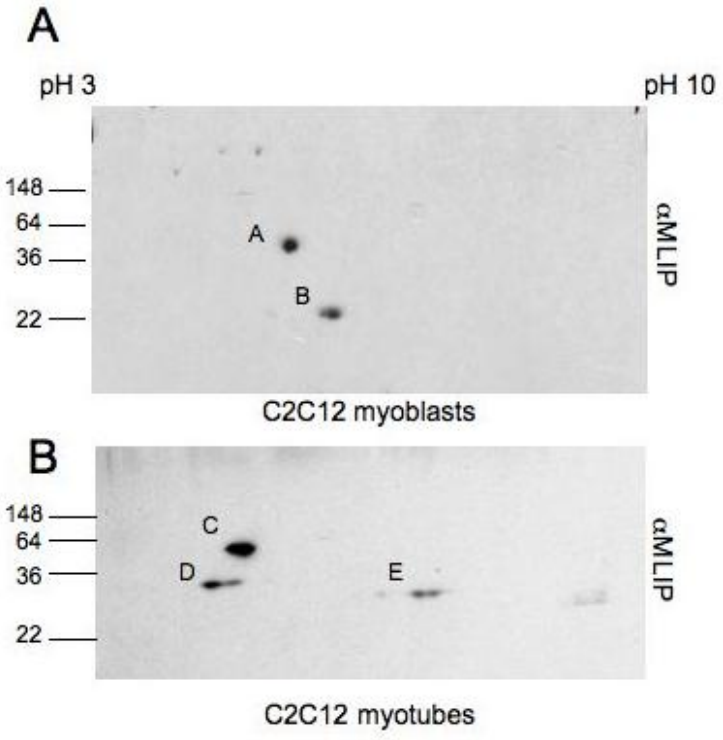

Protein spots on gel	Isoelectric point	MW (kDa)
A	5.5	48
B	6.1	29
C	4.7	44
D	4.3	31
E	6.8	26

Figure 10: Association of identified splice variants to protein bands.

HL-1 cell lysates were probed with a MLIP antibody. The molecular weight of the protein bands were estimated and associated with the splice variants identified through cloning.

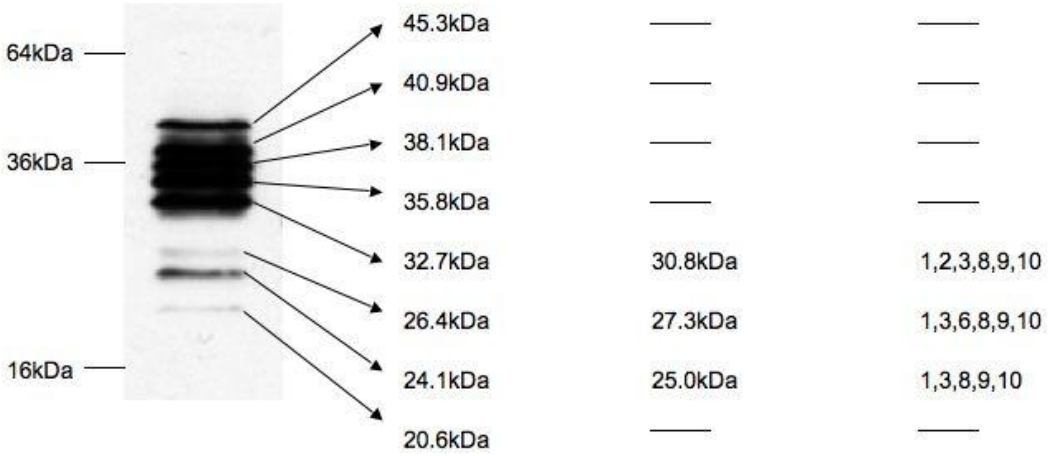
Molecular weight-Western
Splice variant identified through cloning (Molecular Weight)
Putative splice variant exons
64kDa
36kDa
16kDa
45.3kDa
40.9kDa
38.1kDa
35.8kDa
32.7kDa
26.4kDa
24.1kDa
20.6kDa
30.8kDa
27.3kDa
25.0kDa
1,2,3,8,9,10
1,3,6,8,9,10
1,3,8,9,10

MLIP has a single 5' and 3' untranslated region in the mouse heart

To explore the possibility of alternative 5' and 3' untranslated regions, 5' and 3' Rapid Amplification of Complementary DNA ends (RACE) was performed. Heart RNA was selected for the template as immunoblotting reveals this tissue to contain the most MLIP isoforms (**Figure 7**).

For 5'RACE, RNA was extracted from mouse adult heart and reverse transcribed using a primer to MLIP. Two sets of cDNA were synthesized, the first using a primer designed to exon 1 and the second designed to exon 3. The cDNA was subsequently poly(A) tailed and then subjected to PCR. A portion of the PCR product was then used as a template for a final nested PCR. Once again two sets of PCR reactions were set up in each step, one using primers to exon 1 and the second to exon 3. The PCR products were TA TOPO cloned, transformed and sequenced. Out of forty-eight clones analyzed, seventeen extended to the 5' untranslated region and a single 5'untranslated region was uncovered, corresponding to that found in the UCSC Genome Browser (Kent WJ, Sugnet CW, Furey TS, Roskin KM, Pringle TH, Zahler AM, Haussler D. The human genome browser at UCSC. *Genome Res.* 2002 Jun;12(6):996-1006)(**Figure 11**). In the mouse this 5'UTR is localized to chromosome 9q bases 77,195,570 to 77,195,677. Our lab has not yet performed 5'RACE using human tissues, however the UCSC Genome Browser Bioinformatics site (Kent WJ, Sugnet CW, Furey TS, Roskin KM, Pringle TH, Zahler AM, Haussler D. The human genome browser at UCSC. *Genome Res.* 2002 Jun;12(6):996-1006) predicts a single 5'UTR which spans bases 53,883,714 to 53,883,827 on chromosome 6.

For 3'RACE, RNA was extracted from mouse adult heart and reverse transcribed using an oligo-dT anchor primer. Amplification of the cDNA was done using a primer to exon 1, another to exon 3, and a third reaction with a primer designed to exon 8. The PCR products were TA TOPO cloned, transformed and sequenced. Out of fourty-eight clones analyzed, thirteen extended to a single 3' untranslated region. In mouse, MLIP's 3'UTR does not contain the most common form of poly-adenylation signal (PAS) which is AAUAAA (Chatterjee and Pal, 2009). MLIP's 3'UTR spans nucleotides 76,949,892 to 76,950,197 and contains the hexamer AAGAAA that could act as a poly-adenylation signal. Although our lab has not performed 3' RACE of MLIP on human samples, the UCSC Genome Browser Bioinformatics site (Kent WJ, Sugnet CW, Furey TS, Roskin KM, Pringle TH, Zahler AM, Haussler D. The human genome browser at UCSC. *Genome Res.* 2002 Jun;12(6):996-1006) predicts two alternative 3'UTRs. The first 3'UTR spans nucleotides 54,080,000 - 54,082,882 on chromosome 6 and contains the PAS AAUAAA as well as a large number of polyadenylation signal variants. The second MLIP 3'UTR in humans, spans nucleotides 54,130,753 to 54,131,074 and harbors the PAS AAUAAA, but does not contain any variant of this hexamere.

Figure 11: In the adult mouse heart, MLIP has a single 5' Untranslated Region.

Determined through 5' Rapid Amplification of Complementary DNA ends. Highlighted in orange is the sequence submitted through the blat algorithm using the UCSC Genome Browser Bioinformatics site (Kent WJ, Sugnet CW, Furey TS, Roskin KM, Pringle TH, Zahler AM, Haussler D. The human genome browser at UCSC. *Genome Res.* 2002 Jun;12(6):996-1006). The purple box outlines the putative 5'UTR of MLIP.

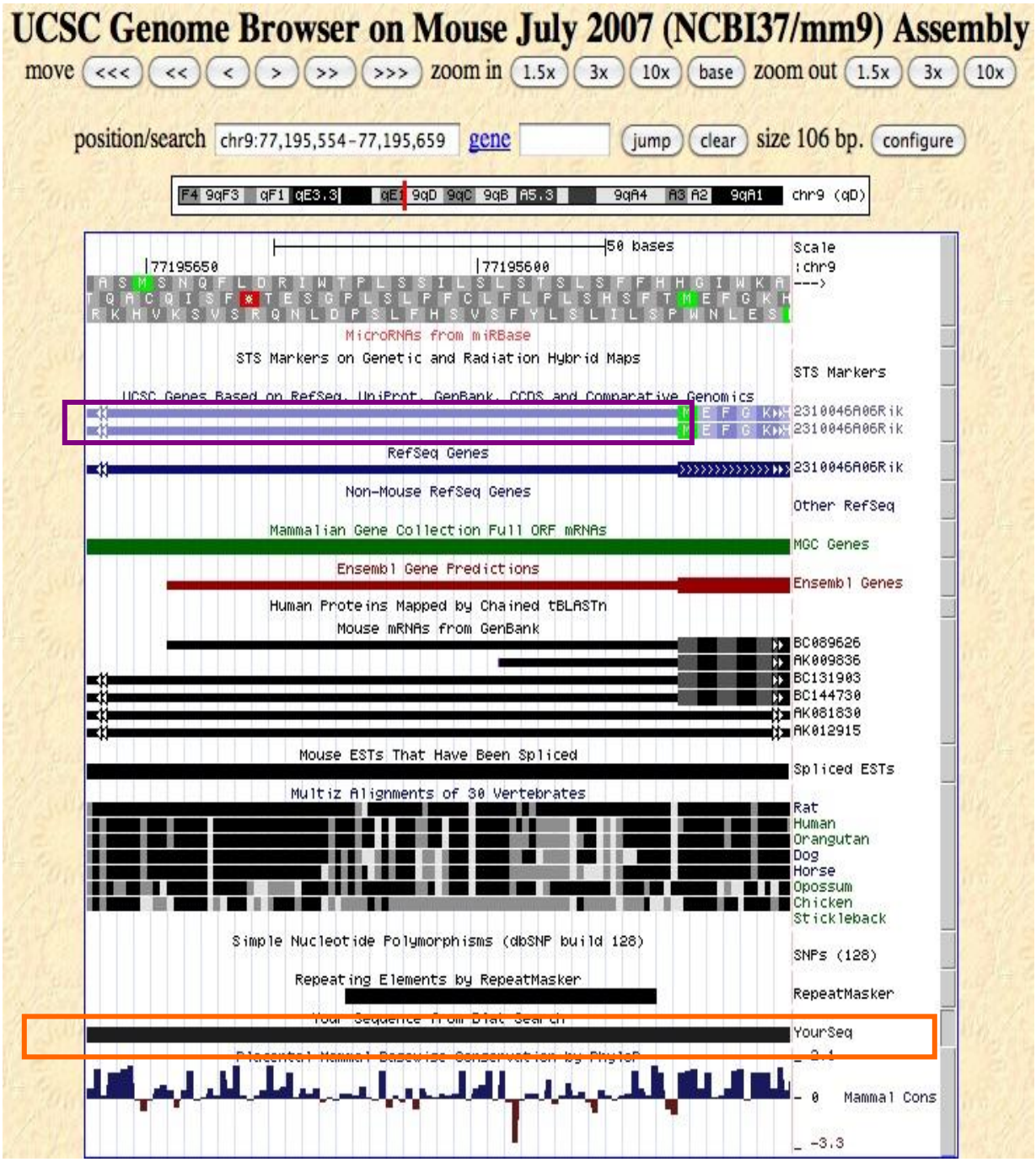
UCSC Genome Browser on Mouse July 2007 (NCBI37/mm9) Assembly
move <<< << < > >> >>> zoom in 1.5x 3x 10x base zoom out 1.5x 3x 10x
position/search chr9:77,195,554-77,195,659 gene jump clear size 106 bp. configure
F4 9qF3 qF1 qE3.3 qE1 9qD 9qC 9qB A5.3 9qA4 A3 A2 9qA1 chr9 (qD)
50 bases
77195650
77195600
Scale
:chr9
MicroRNAs from miRBase
STS Markers on Genetic and Radiation Hybrid Maps
STS Markers
UCSC Genes Based on RefSeq, UniProt, GenBank, CCDS and Comparative Genomics
2310046A06Rik
2310046A06Rik
RefSeq Genes
2310046A06Rik
Non-Mouse RefSeq Genes
Other RefSeq
Mammalian Gene Collection Full ORF mRNAs
MGC Genes
Ensembl Gene Predictions
Ensembl Genes
Human Proteins Mapped by Chained tBLASTn
Mouse mRNAs from GenBank
BC089626
AK009836
BC131903
BC144730
AK081830
AK012915
Mouse ESTs That Have Been Spliced
Spliced ESTs
Multiz Alignments of 30 Vertebrates
Rat
Human
Orangutan
Dog
Horse
Opossum
Chicken
Stickleback
Simple Nucleotide Polymorphisms (dbSNP build 128)
SNPs (128)
Repeating Elements by RepeatMasker
RepeatMasker
YourSeq
Mammal Cons

MLIP contains a highly conserved SUMOylation consensus sequence

In order to investigate the possibility of post-translational modification, putative post-translation modification sites were examined. MLIP contains five highly conserved regions of homology, (Ahmady et al., 2011)[1] one of which includes a putative SUMOylation sequence, as illustrated in **Figure 12**. The consensus sequence for SUMOylation is ΨKXE/D, (Sampson et al., 2001) where Ψ is a large hydrophobic residue and X can be any amino acid. In MLIP this sequence is FKAE and resides within exon 3.

[1] Elmira Ahmady, Shelley A. Deeke, Seham Rabaa, Lara Kouri, Laura Kenney, Alexandre F. R.Stewart & Patrick G. Burgon (2011). Identification of a novel Muscle Enriched A-Type Lamin Interacting Protein (MLIP). *Under 2nd revision JBC April 2011*

Figure 12: Highly Conserved Predicted SUMOylation site within Exon 3 of MLIP

In red is the SUMOylation consensus sequence ΨKXE/D (Ψ= a large hydrophobic residue; X =any amino acid). Asterix represents conservation with MLIP *Homo sapiens*. Alignment was performed using MegAlign.

Homo sapiens	**Q**	**S**	**D**	**L**	**F**	**K**	**A**	**E**	**Y**	**V**	**L**
P.troglodytes	*	*	*	*	*	*	*	*	*	*	*
Macaca mulatta	*	*	*	*	*	*	*	*	*	*	*
R.norvegicus	K	G	*	*	*	*	*	*	*	*	F
Mus musculus	K	G	*	*	*	*	*	*	*	*	F
Canis lupus familar	*	*	*	*	*	*	*	*	*	*	F
Equuscaballus	*	*	*	*	*	*	*	*	*	*	F
Bos Taurus	*	*	*	*	*	*	*	*	*	*	F
M.domestic	*	*	*	*	*	*	*	*	*	*	F
Gallus gallus	E	N	*	*	*	*	*	*	F	I	*

Recombinant MLIP does not undergo in vitro post-translational modification by SUMO1 or SUMO2

To address the possibility of post-translational modification by SUMO, an *in vitro* SUMOylation assay was performed using a recombinant MLIP protein. The MLIP splice variant containing exons 1, 3, 8, 9 and 10 was subcloned into the His-tag vector pET100D, expressed in *E. coli* and subsequently purified using a His Trap column (**Figure 13**). This splice variant has a theoretical molecular weight of 25kDa and with the addition of the linker and His-tag the theoretical molecular weight adds up to 30kDa, which is in accordance with the rMLIP generated (**Figure 13**). A mock control purification was also performed in order to account for contaminant proteins present from the purification process that could undergo SUMOylation (**Figure 14**).

The recombinant MLIP protein or the mock control was incubated with the SUMO E1 activating enzyme, the SUMO E2 conjugating enzyme, either SUMO1 or SUMO2, as well as in the presence or absence of ATP. Excluding ATP demonstrates that the reaction is specific to the SUMOylation cascade, as ATP is required for the activation of the E1 activating enzyme (Desterro et al., 1997; Johnson, et al., 1997). As shown is **Figure 15**, recombinant MLIP is not a substrate for SUMO1 or SUMO2, as there are no larger molecular forms of MLIP present on the MLIP blot. In addition, the SUMO immunoblotting pattern is almost identical between the mock control and the sample containing the recombinant MLIP protein. The SUMO1 and SUMO2 staining of larger molecular proteins arises from contaminant proteins present from the purification process as they are present in the mock control sample.

Figure 13: Expression and purification of recombinant MLIP.

The MLIP splice variant containing exons 1, 3, 8, 9, 10 was expressed in *E. coli* and purified using a His Trap column. Purification fractions were resolved on a polyacrylamide gel and subsequently immunoblotted for MLIP (**A**) or stained with Commassie (**B**). Elution # 8, 9 and 10 were pooled and concentrated to yield the final recombinant MLIP protein fraction used for *in vitro* SUMOylation, Coomassie staining (**C**) or immunoblotting for MLIP (**D**).

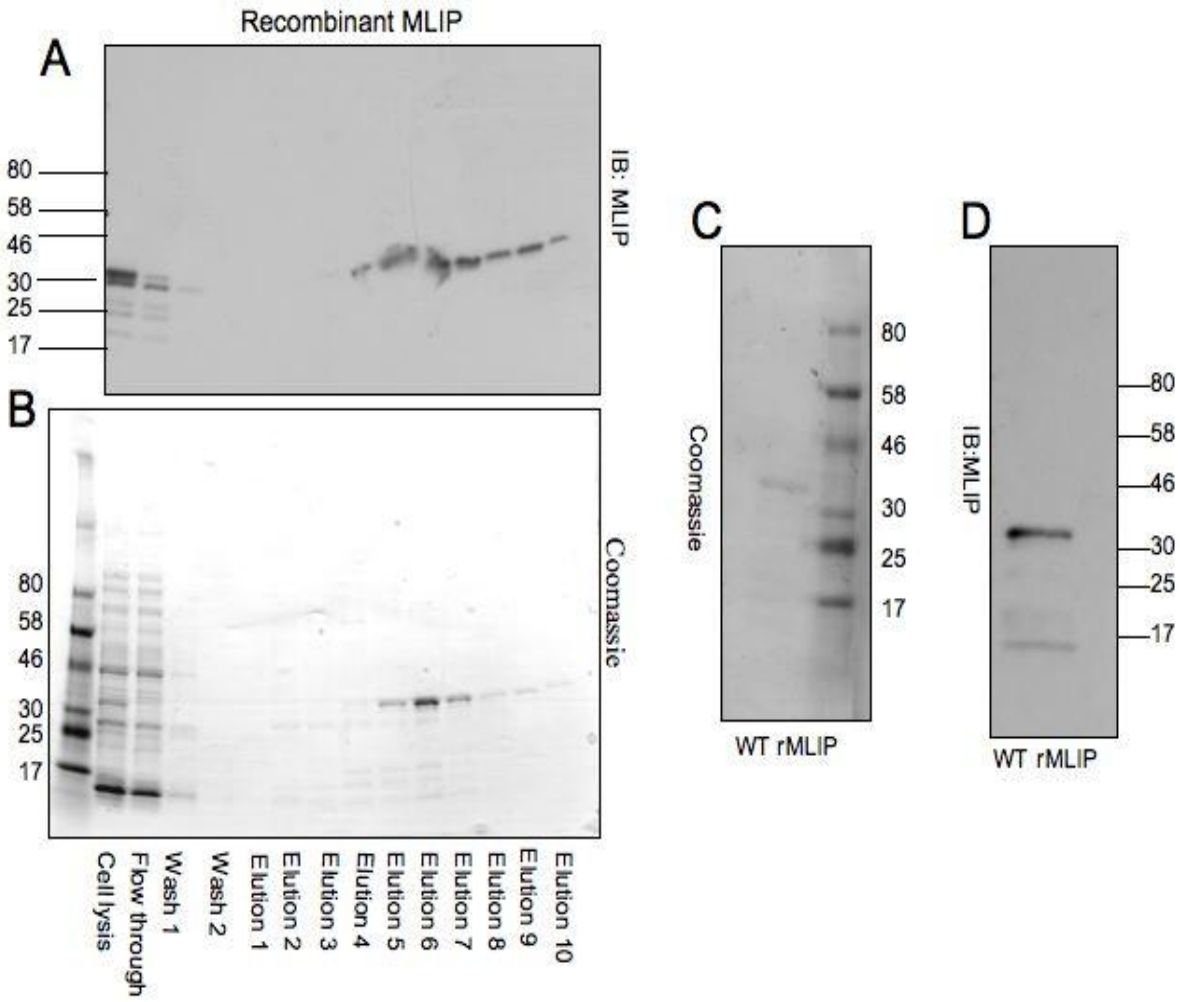
Recombinant MLIP
A
80
58
46
30
25
17
IB: MLIP
B
80
58
46
30
25
17
Coomassie
Cell lysis
Flow through
Wash 1
Wash 2
Elution 1
Elution 2
Elution 3
Elution 4
Elution 5
Elution 6
Elution 7
Elution 8
Elution 9
Elution 10
C
Coomassie
80
58
46
30
25
17
WT rMLIP
D
IB:MLIP
80
58
46
30
25
17
WT rMLIP

Figure 14: Mock control expression and purification.

The mock control vector was expressed in *E. coli* and purified using a His Trap column. Purification fractions were resolved on a polyacrylamide gel and subsequently immunoblotted for MLIP (**A**) or stained with Commassie (**B**). Elution # 8, 9 and 10 were pooled and concentrated to yield the final mock control fraction used for *in vitro* SUMOylation, Coomassie staining (**C**) or immunoblotting for MLIP (**D**).

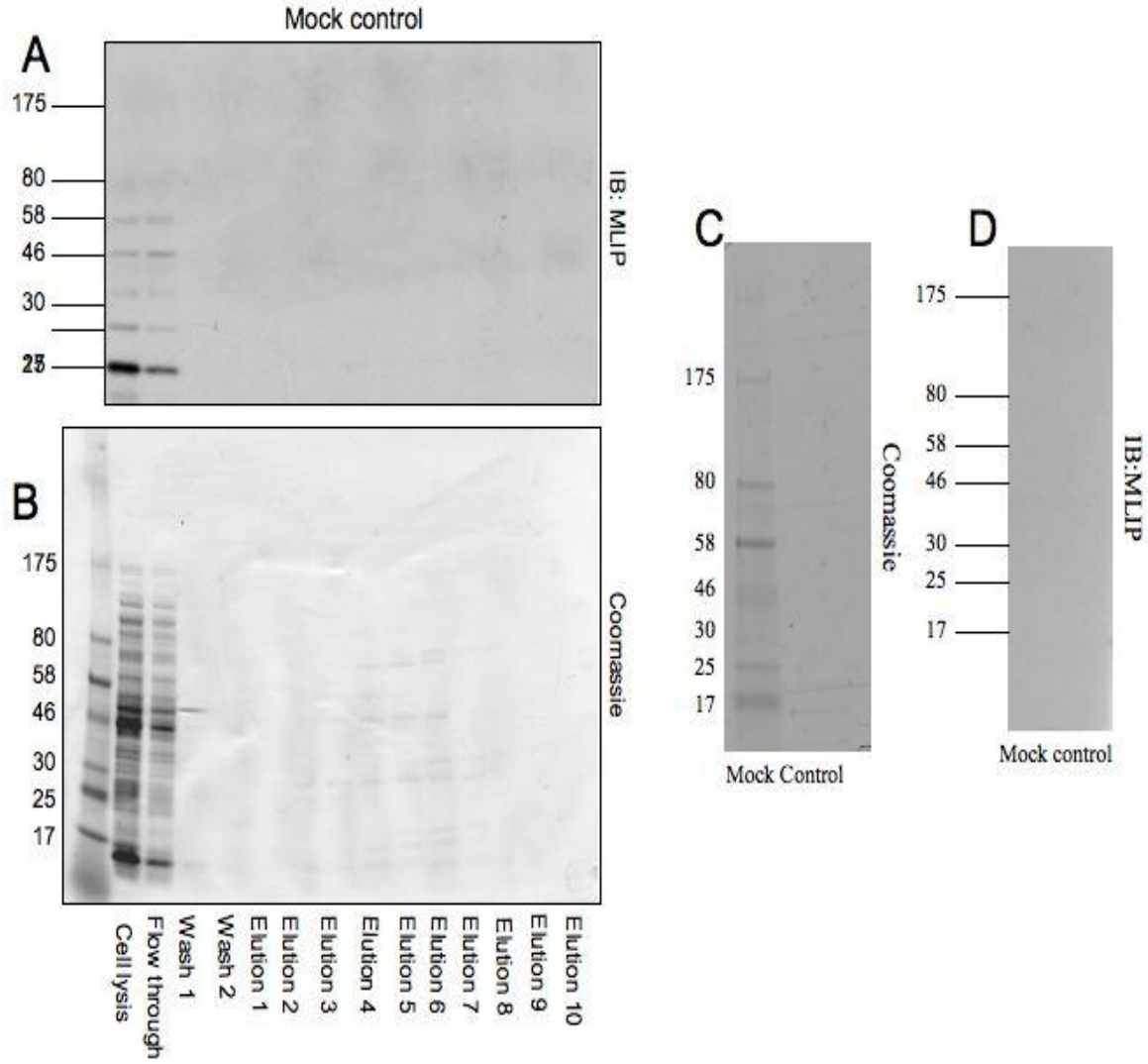
Mock control
A
175
80
58
46
30
25
IB: MLIP
B
175
80
58
46
30
25
17
Coomassie
Cell lysis
Flow through
Wash 1
Wash 2
Elution 1
Elution 2
Elution 3
Elution 4
Elution 5
Elution 6
Elution 7
Elution 8
Elution 9
Elution 10
C
175
80
58
46
30
25
17
Coomassie
Mock Control
D
175
80
58
46
30
25
17
IB:MLIP
Mock control

Figure 15: MLIP is not modified *in vitro* by SUMO1 or SUMO2.

Recombinant MLIP or the mock control was incubated with the SUMO E1 activating enzyme, the SUMO E2 conjugation enzyme, SUMO1 (**A**) or SUMO2 (**B**), and either in the presence or absence of ATP to assess for *in vitro* SUMOylation. Omitting ATP demonstrates that the reaction arises from the SUMOylation cascade, as ATP is required to activate the E1 enzyme.

A

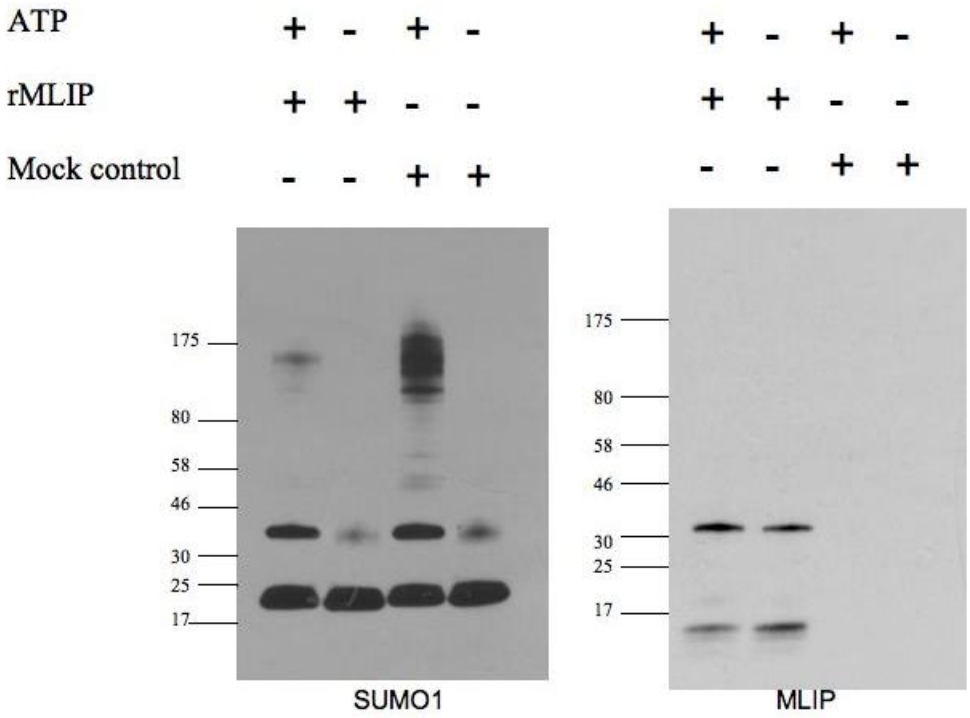
ATP
rMLIP
Mock control
+ - + -
+ + - -
- - + +
175
80
58
46
30
25
17
SUMO1
MLIP

B

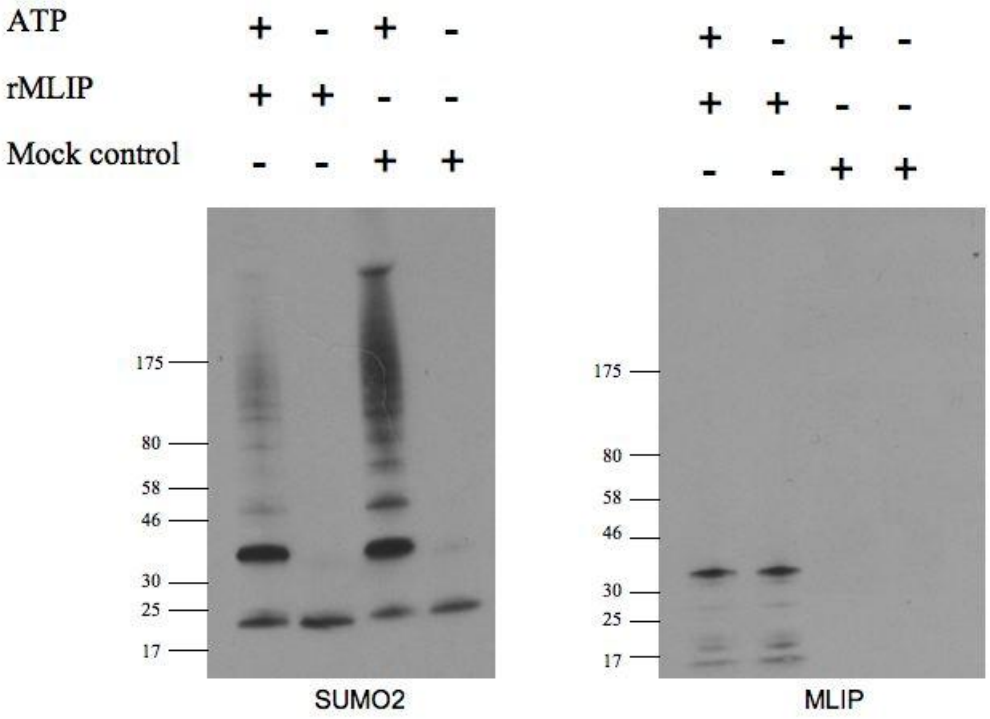
ATP
rMLIP
Mock control
+ - + -
+ + - -
- - + +
175
80
58
46
30
25
17
SUMO2
MLIP

Endogenous MLIP is not modified by SUMO1 or SUMO2 in HL-1 cells

There are no MLIP homologues in bacteria and therefore there is concern as to whether the recombinant protein is properly folded. It has been demonstrated that the lysine residue on the target protein that is modified by SUMO, enters the catalytic pocket of the E2 conjugating enzyme and that the hydrophobic and acidic residues interact with the surface of the E2 conjugating enzyme, (Bernier-Villamor et al., 2002) hence the structure of the target protein plays an important role. In order to address this concern, immunoprecipitation of endogenous MLIP was performed on HL-1 cell lysates under normal conditions, **Figure 16**. Following immunoprecipitation, blots were probed with SUMO1, SUMO2 or MLIP. Probing for MLIP after immunoprecipitation was to ensure that our MLIP antibody was suitable for immunoprecipitation. Pre-immune serum from the rabbit from which the antibody was generated was used as a negative control. As seen in **Figure 16**, there is no difference between the pre-immune serum and MLIP immunoprecipitation, hence MLIP does not undergo SUMOylation by SUMO1 or SUMO2 in HL-1 cells.

Figure 16: Endogenous MLIP is not a substrate of SUMO1 or SUMO2 in HL-1 cells.

(**A**)Extracts of HL-1 cardiac muscle cells underwent immunoprecipitation using an MLIP antibody or pre-immune serum and subsequently immunoblotted using a SUMO1, SUMO2 or MLIP antibody. HL-1 cells lysates were also probed for MLIP. (**B**) HL-1 cell lysates probed with a SUMO1 or SUMO2 antibody.

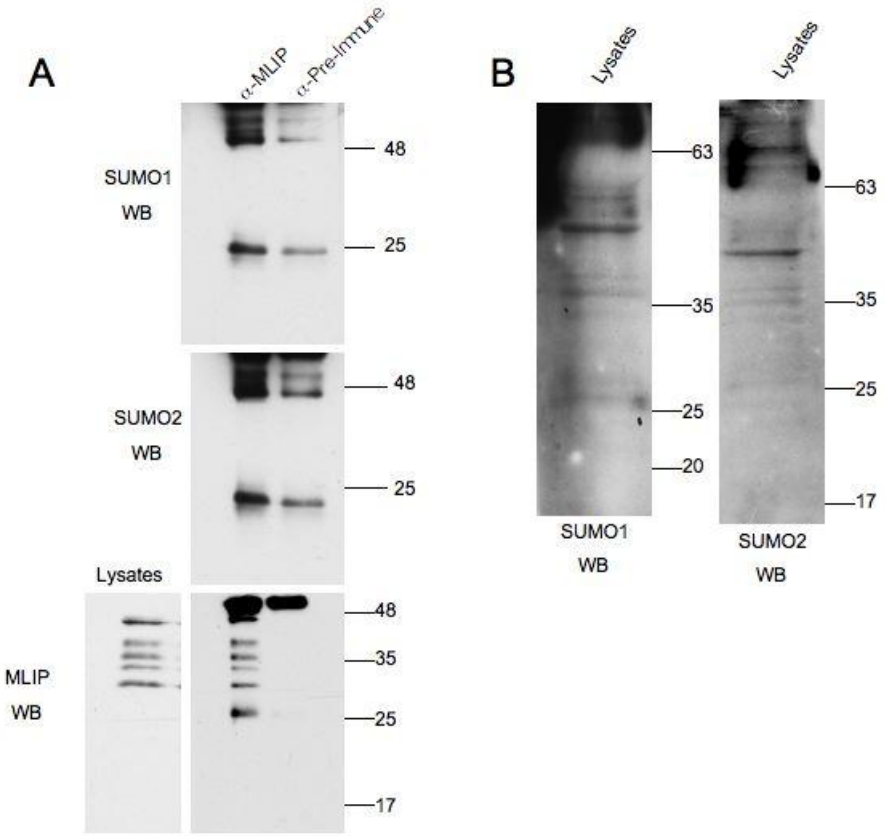
A
α-MLIP
α-Pre-Immune
SUMO1
WB
48
25
SUMO2
WB
48
25
Lysates
MLIP
WB
48
35
25
17
B
Lysates
Lysates
63
35
25
20
SUMO1
WB
63
35
25
17
SUMO2
WB

Chapter 4:
Discussion

Discussion:

As part of these studies, the isoforms of a novel Muscle-enriched A-type Lamin-Interacting Protein (MLIP) were investigated using an assortment of molecular biology techniques. MLIP was originally identified as an interactor of A-type Lamins with the intention of discerning at least in part, the perplexing mechanisms of Laminopathies (Ahmady et al., 2011)[1]. Mutations within A-type Lamins can give rise to a diverse array of disease, affecting a wide range of tissues, while the mechanism still remains poorly understood (Worman et al., 2009). Whether MLIP plays a role in the pathogenesis of laminopathies remains elusive. Through detailed analysis of the GenBank database, it was established that MLIP does not display any substantial similarity to any gene and is present exclusively in amniotes, perhaps attributing to the complexity of higher organisms (Ahmady et al., 2011)[1]. By means of immunoblotting experiments it was clear that more than one MLIP isoform existed, hence the overall aim of this thesis was to identify MLIP's isoforms.

Immunoblotting for MLIP in various mouse tissues demonstrated that MLIP seems to be enriched in brain, heart and skeletal muscle (**Figure 7**) which is consistent with Northern blot results which show that MLIP is mainly associated with these tissues (Ahmady et al., 2011)[1]. Also in agreement with these results, an analysis in GEO profiles (**Supplemental Figure 3**) demonstrates a similar trend, in which MLIP is enriched in heart, muscle, diaphragm and brain (NCBI, GEO profiles, record GDS3142/ 14253059_at/ 2310046A06Rik). Immunoblotting for MLIP in various human tissues showed it to be

[1] Elmira Ahmady, Shelley A. Deeke, Seham Rabaa, Lara Kouri, Laura Kenney, Alexandre F. R.Stewart & Patrick G. Burgon (2011). Identification of a novel Muscle Enriched A-Type Lamin Interacting Protein (MLIP). *Under 2nd revision JBC April 2011*

enriched in the heart and skeletal muscle which is in accordance with previous Northern blotting experiments that demonstrate MLIP to be highly expressed in skeletal muscle and heart with low levels seen in the liver (Ahmady et al., 2011)[1]. Consistent with these results, an analysis in GEO profiles (**Supplemental Figure 4**) shows MLIP to be highly expressed in human heart and skeletal muscle, with low level expression in the liver, spinal cord and very low expression in brain. (NCBI, GEO profiles, record GDS424/ 54910_at/ C6orf142). In both human and mouse, MLIP is enriched in striated muscle. The type of MLIP isoform expression differs between tissues, however the reason for this difference in expression remains to be elucidated.

The cloning strategy demonstrated that MLIP's alternative splicing is tissue-dependent. Whether the stability, subcellular localization, function or interacting partners of the different isoforms is similar remains to be determined. Exons 4, 5, 7 and 11 were not detected in the cells analyzed, however exons 5, 7 and 11 were found when analyzing the 3' RACE sequences from adult mouse heart tissue. Although exon 4 was not encountered through my cloning experiments, this exon has been detected in other PCR amplification studies (Ahmady et al., 2011)[1].

The cloning strategy identified four splice variants in HL-1 cells with the following molecular weights; 10kDa, 25kDa, 27kDa and 30kDa. The last three splice variants are in accordance with the bands observed in HL-1 cell immunoblotting for MLIP (**Figure 10**). The 10kDa splice variant however, has not been detected via immunoblottting. Considering the size of this protein, it is possible that detection has not been possible due to the

[1] Elmira Ahmady, Shelley A. Deeke, Seham Rabaa, Lara Kouri, Laura Kenney, Alexandre F. R.Stewart & Patrick G. Burgon (2011). Identification of a novel Muscle Enriched A-Type Lamin Interacting Protein (MLIP). *Under 2nd revision JBC April 2011*

conditions used for immunoblotting. For example, a smaller membrane pore size could remove the risk of the protein passing through the aforementioned membrane. Alternatively it is also possible that this transcript is not translated into protein.

Myoblasts isolated from a rodent's hind limb contained an MLIP splice variant (exons 1, 3, 8, 9, 10) that differed from that of the myotubes (exons 1, 2, 3, 8, 9, 10) from which the myoblast differentiated into, upon serum removal. This observation was not mimicked in C2C12 myoblasts and myotubes, as they contained the same MLIP splice variant. This result could represent an instance in which the C2C12 immortalized mouse myoblast cell line does not mirror normal tissue.

Through 5' RACE, it was established that in the adult mouse heart, MLIP contains a single 5' untranslated reagion. An alternative transcription start site (TSS) for C6orf142 (MLIP) has recently been described for the human brain (Wakamatsu et al., 2009). In this study, more than eleven thousand full-length human cDNAs were identified and analyzed for alternative splicing. Many features of the 5'UTR participate in determining gene expression, one of which is the presence of upstream open reading frames (uORF) (Chatterjee and Pal, (2009). In both mouse and human, an uORF can be found in the 5'UTR of MLIP, however whether the presence of an uORF influences MLIP's gene expression remains to be tested. In mouse, the uORF gives rise to a 6 amino acid peptide, the entire sequence residing within the 5'UTR. In humans, the peptide consists of 34 amino acids, with the termination codon residing in the first exon of MLIP.

Two-dimensional electrophoresis was performed on C2C12 myoblasts as well as C2C12 myotubes to gain further information on MLIP's protein expression. As C2C12 cells undergo myogenesis an additional MLIP protein band appears by immunoblotting, however

this band was not identified through cloning and therefore whether this protein band is a result of post-translational modification or alternative splicing is not known. Whether this MLIP isoform plays a role in stimulating myogenesis or whether its expression is induced by myogenesis is unknown. Lamin A has been shown to play an important role in myogenesis (Favreau et al., 2004). C2C12 myoblast cells overexpressing a lamin mutant (R453W) demonstrated hindered myotube formation compared to cell expressing wild-type lamin A (Favreau et al., 2004). Interestingly, previous experiments demonstrated a possible role for MLIP in myogenesis, as knocking down MLIP using shRNAmir constructs seemed to impair proper myotube formation (Ahmady M.Sc. thesis, 2010, University of Ottawa). In addition, ChIP-on-chip experiments unveiled several putative MLIP targets that play a role in muscle development, commitment and differentiation (Ahmady M.Sc. thesis, 2010, University of Ottawa).

The number of MLIP protein bands observed through immunoblotting cannot be accounted for by the number of splice variants identified to date. Although peptide neutralization immunoblotting studies have been done (**Supplemental Figure 5**), immunoblotting of MLIP knock out mice tissues has yet to be done, as these mice are currently being developed. This important experiment would reveal whether any of the immunoblotting bands are due to non specific binding. MLIP heterozygous knock out mice are presently under examination in our lab and we hope to study the MLIP homozygous knock out mice in the near future. To date, no MLIP homozygote null mouse has been observed; suggesting the loss of MLIP is embryonically lethal. Another future experiment that could reveal the identity of the unknown isoforms would be mass spectrometry. Since

our antibody appears to perform excellently for immunoprecipitations (**Figure 16**, panel A), the individual bands could be excised and submitted for mass spectrometry.

When examining MLIP's conservation biology and putative post-translational sites, a highly conserved putative SUMOylation sequence was found (**Figure 12**). Lamin A has been shown to undergo modification by SUMO2. Mutating the lysine residue within the SUMOylation site of lamin A leads to abnormal subcellular localization (Zhang and Sarge, 2008). The mutations E203G and E203K in lamin A cause dilated cardiomyopathies and these two mutants were examined for their ability to undergo SUMOylation, which was decreased, possibly offering an explanation for the disease (Zhang and Sarge, 2008). In order to examine whether MLIP can be modified by SUMO, a recombinant MLIP protein was synthesized and purified and subsequently used for an *in vitro* SUMOylation assay. Recombinant MLIP did not undergo SUMOylation by either SUMO1 or SUMO2, however there was concern as to whether the recombinant MLIP protein is folded into its proper three-dimensional structure, hence immunoprecipitation was performed on endogenous MLIP in HL-1 cells. MLIP does not appear to be modified *in vivo* by SUMO1 or SUMO2.
It has been shown that the level of SUMOylation of a target protein may be insufficient to be detectable by immunoprecipitation of the endogenous protein (Tatham et al., 2009). Previous studies show that for many SUMO target proteins, the amount of protein which undergoes SUMO modification under steady state conditions is low (Tatham et al., 2009, Vertegaal et al., 2006). In order to address this concern, studies have either treated with agents such as MG132, subjected cells to heat-shock, or overexpressed members of the SUMOylation cascade or the target protein to overcome this problem, however any one of these methods increase the potential for false-positive results (Tatham et al., 2009). It is not

uncommon for a protein to contain a SUMOylation consensus sequence but not undergo post-translational modification by SUMO. Thirty-three per cent of characterized proteins contain the sequence ΨKXE (Yang et al., 2006). One study assessed the ability of 39 proteins, which contain the SUMOylation consensus sequence (ΨKXE), to undergo modification by SUMO1. Out of the 39 proteins assessed only 14 were post-translationnaly modified by SUMO1 (Wilkinson et al., 2008).

Lamin A/C is not expressed in undifferentiated mouse and human embryonic stem cells, hence the lack of A-type lamin expression is a marker for undifferentiated embryonic stem cells (Constantinescu et al., 2006). The commitment of a cell to a specific cell fate transpires before the expression of Lamin A can be detected (Rober et al., 1989). Lamin A/C has been suggested to limit the ability of a cell to modify its' phenotype in response to the environment (Rober et al., 1989). MLIP's tissue dependent expression may suggest that it too plays a role in plasticity. Whether MLIP is the result of acquired cell type or plays a role in the acquisition of the cell fate remains elusive. Interestingly, a gene profiling expression analysis performed by Haslett et al., (**Supplemental Figure 1**) demonstrated that MLIP expression is decreased in patients suffering from DMD compared to healthy subjects. In this study, tissue biopsies were collected from quadricep skeletal muscle. Another study performed by Barth et al., (**Supplemental Figure 2**) showed an increase in C6orf142 (MLIP) expression in DCM compared to patients with non-failing hearts. This study examined septal myocardial tissue samples. There are currently no profiling studies of MLIP expression in Partial lipodystrophy or Charcot-Marie-Tooth.

Future Direction

The PhosphoSitePlus (Produced by 3rd Millennium©2003-2011 Cell Signaling Technology, Inc.) is a database in which mass spectrometry is deposited. According to this database, MLIP is phosphorylated on three different serine residues, two of which are highly conserved. The cluster of unidentified bands present between 35kDa and 40kDa (**Figure 10**) could be due to phosphorylation of MLIP. To test this hypothesis site-directed mutagenesis would be performed, mutating the serine residues, and subsequent immunoblotting would be performed to assess whether the cluster of unidentified bands disappears. These mutants would also be transfected into cells and subsequently visualized by fluorescent microscopy to assess whether MLIP's subcellular localization is influenced by phosphorylation. Whether all of MLIP's isoforms display the same subcellular localization has yet to be tested. Future experiments include separating nuclear and cytoplasmic fractions and immunoblotting for MLIP to assess whether the isoforms differ between cellular fractions.

Conclusion

In this work, several of the MLIP isoforms have been identified, although many still remain unknown. MLIP's expression differs between tissues and MLIP is subjected to extensive tissue-dependent alternative splicing. Although MLIP does not appear to be a substrate for SUMO, it remains to be tested whether it undergoes other post-translational modifications. MLIP's function has yet to be defined, however preliminary experiments in our laboratory and MLIP's association with lamin suggest that it may play a role in tissue differentiation.

Appendix

Figure S 1: GEO profiles. Expression profile analysis of human MLIP (C6orf142) in normal and in Duchenne muscular dystrophy (DMD) patients.

Biopsies from quadriceps skeletal muscle tissue.
NCBI, GEO profiles, record GDS610 / 54910_at / C6orf142 / Homo sapiens

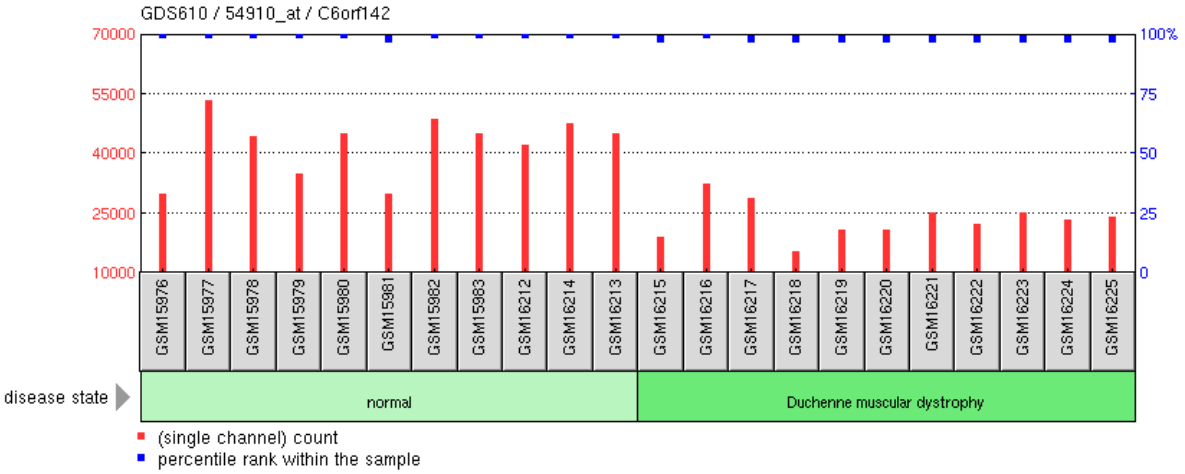
GDS610 / 54910_at / C6orf142
70000
55000
40000
25000
10000
100%
75
50
25
0
GSM15976
GSM15977
GSM15978
GSM15979
GSM15980
GSM15981
GSM15982
GSM15983
GSM16212
GSM16214
GSM16213
GSM16215
GSM16216
GSM16217
GSM16218
GSM16219
GSM16220
GSM16221
GSM16222
GSM16223
GSM16224
GSM16225
disease state
normal
Duchenne muscular dystrophy
(single channel) count
percentile rank within the sample

Figure S 2: GEO profiles. Expression profile analysis of MLIP (C6orf142) in patients with non-failing heart and patients with Dilated Cardiomyopathy.

Septal myocardial tissue was collected for analysis.
NCBI, GEO profiles, record GDS2206 / RZPDp1096H094D / C6orf142 / Homo sapiens

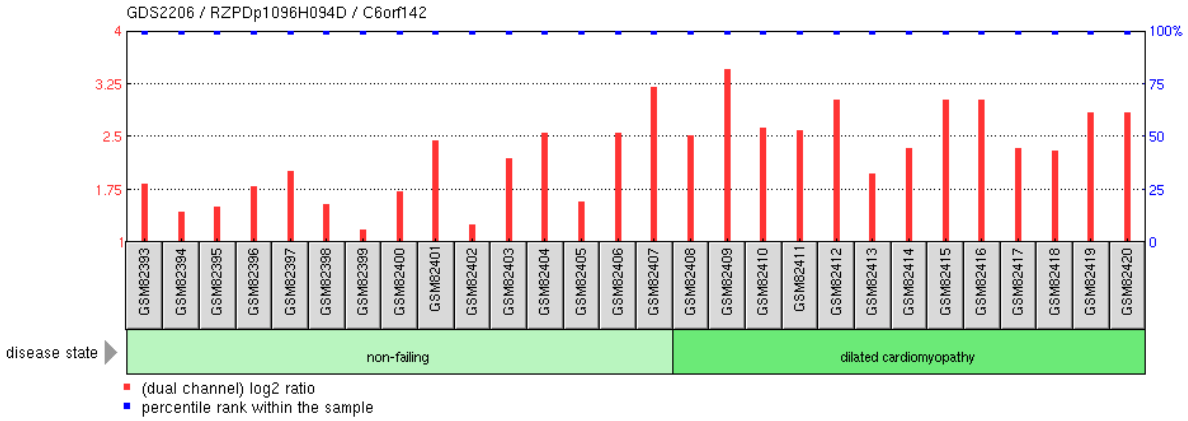
GDS2206 / RZPDp1096H094D / C6orf142
4
3.25
2.5
1.75
1
100%
75
50
25
0
GSM82393
GSM82394
GSM82395
GSM82396
GSM82397
GSM82398
GSM82399
GSM82400
GSM82401
GSM82402
GSM82403
GSM82404
GSM82405
GSM82406
GSM82407
GSM82408
GSM82409
GSM82410
GSM82411
GSM82412
GSM82413
GSM82414
GSM82415
GSM82416
GSM82417
GSM82418
GSM82419
GSM82420
disease state
non-failing
dilated cardiomyopathy
(dual channel) log2 ratio
percentile rank within the sample

Figure S 3: GEO profiles. Expression profile analysis of mouse MLIP (2310046A06Rik) in normal tissues.

NCBI, GEO profiles, record GDS3142/ 14253059_at/ 2310046A06Rik

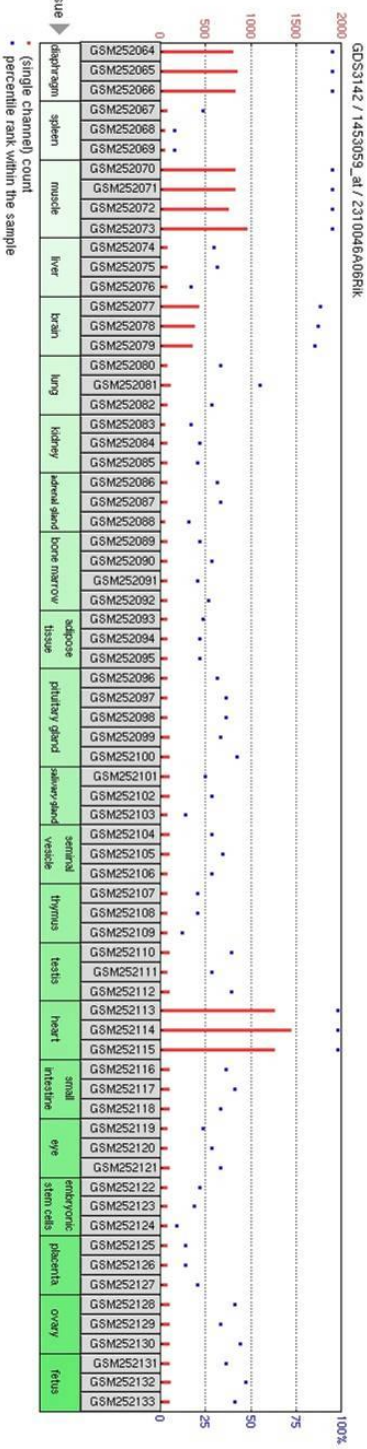
GDS3142 / 1453059_at / 2310046A06Rik
tissue
diaphragm
spleen
muscle
liver
brain
lung
kidney
adrenal gland
bone marrow
adipose tissue
pituitary gland
salivary gland
seminal vesicle
thymus
testis
heart
small intestine
eye
embryonic stem cells
placenta
ovary
fetus
GSM252064
GSM252065
GSM252066
GSM252067
GSM252068
GSM252069
GSM252070
GSM252071
GSM252072
GSM252073
GSM252074
GSM252075
GSM252076
GSM252077
GSM252078
GSM252079
GSM252080
GSM252081
GSM252082
GSM252083
GSM252084
GSM252085
GSM252086
GSM252087
GSM252088
GSM252089
GSM252090
GSM252091
GSM252092
GSM252093
GSM252094
GSM252095
GSM252096
GSM252097
GSM252098
GSM252099
GSM252100
GSM252101
GSM252102
GSM252103
GSM252104
GSM252105
GSM252106
GSM252107
GSM252108
GSM252109
GSM252110
GSM252111
GSM252112
GSM252113
GSM252114
GSM252115
GSM252116
GSM252117
GSM252118
GSM252119
GSM252120
GSM252121
GSM252122
GSM252123
GSM252124
GSM252125
GSM252126
GSM252127
GSM252128
GSM252129
GSM252130
GSM252131
GSM252132
GSM252133
2000
1500
1000
500
0
100%
75
50
25
0
(single channel) count
percentile rank within the sample

Figure S 4: GEO profiles. **Expression profile analysis of human MLIP (C6orf142) in normal tissues.**

(NCBI, GEO profiles, record GDS424/ 54910_at/ C6orf142)

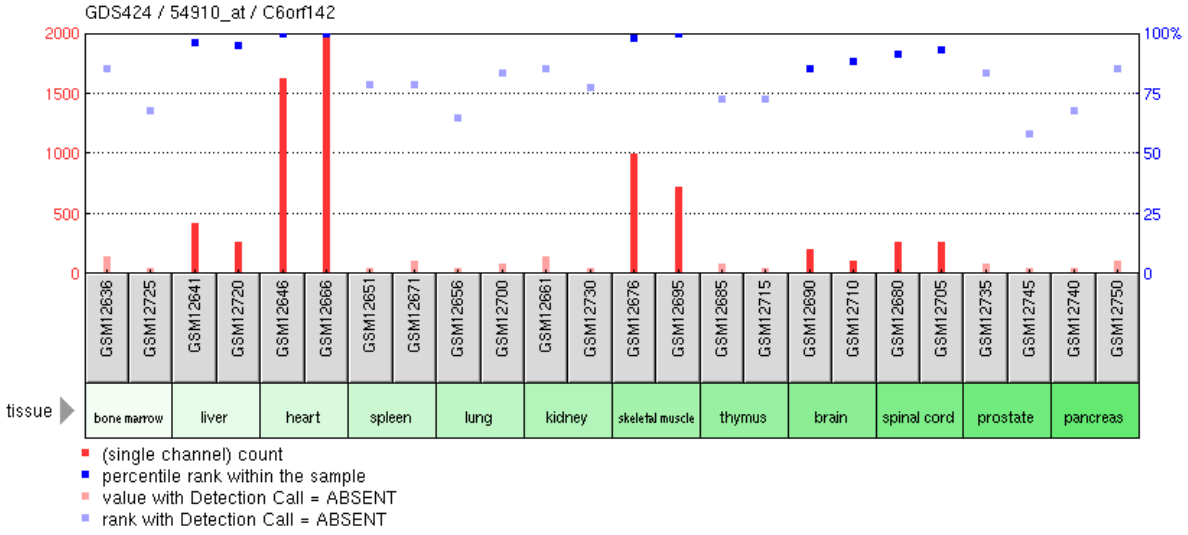
GDS424 / 54910_at / C6orf142
2000
1500
1000
500
0
100%
75
50
25
0
GSM12636
GSM12725
GSM12641
GSM12720
GSM12646
GSM12666
GSM12651
GSM12671
GSM12656
GSM12700
GSM12661
GSM12730
GSM12676
GSM12695
GSM12685
GSM12715
GSM12690
GSM12710
GSM12680
GSM12705
GSM12735
GSM12745
GSM12740
GSM12750
tissue
bone marrow
liver
heart
spleen
lung
kidney
skeletal muscle
thymus
brain
spinal cord
prostate
pancreas
(single channel) count
percentile rank within the sample
value with Detection Call = ABSENT
rank with Detection Call = ABSENT

Figure S 5: Peptide Neutralization

MLIP peptide neutralization of the anti-MLIP sera demonstrates the specificity of the MLIP antibodies in Western blot analysis.

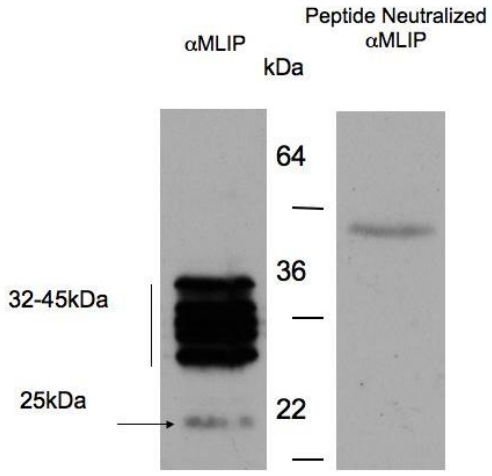
αMLIP
Peptide Neutralized αMLIP
kDa
64
36
22
32-45kDa
25kDa

CONTRIBUTIONS OF COLLABORATORS

The mRNA used for 5’ and 3’ RACE was isolated by Lara Kouri, M.Sc. candidate.

References

Abida, W. M., Nikolaev, A., Zhao, W., Zhang, W., & Gu, W. (2007). FBXO11 promotes the neddylation of p53 and inhibits its transcriptional activity. *Journal of Biological Chemistry, 282*(3), 1797-1804.

Aebi, U., Cohn, J., Buhle, L., & Gerace, L. (1986). The nuclear lamina is a meshwork of intermediate-type filaments. *Nature, 323*(6088), 560-564.

Ahmady, E. (2010). The Functional Role of A-type Lamin Interacting Transcription Factor (LITF) during Skeletal Myogenesis. M.Sc. Thesis, University of Ottawa

Allfrey, V. G., & Mirsky, A. E. (1964). Structural modifications of histones and their possible role in the regulation of RNA synthesis. *Science, 144*(3618), 559.

Ashcroft, M., Kubbutat, M. H. G., & Vousden, K. H. (1999). Regulation of p53 function and stability by phosphorylation. *Molecular and Cellular Biology, 19*(3), 1751-1758.

Azubel, M., Habib, N., Sperling, R., & Sperling, J. (2006). Native spliceosomes assemble with pre-mRNA to form supraspliceosomes. *Journal of Molecular Biology, 356*(4), 955-966.

Barth, A. S., Kuner, R., Buness, A., Ruschhaupt, M., Merk, S., Zwermann, L., et al. (2006). Identification of a common gene expression signature in dilated cardiomyopathy across independent microarray studies. *Journal of the American College of Cardiology, 48*(8), 1610-1617.

Bayer, P., Arndt, A., Metzger, S., Mahajan, R., Melchior, F., Jaenicke, R., et al. (1998). Structure determination of the small ubiquitin-related modifier SUMO-1. *Journal of Molecular Biology, 280*(2), 275-286.

Beaudoing, E., Freier, S., Wyatt, J. R., Claverie, J. -., & Gautheret, D. (2000). Patterns of variant polyadenylation signal usage in human genes. *Genome Research, 10*(7), 1001-1010.

Beck, L. A., Hosick, T. J., & Sinensky, M. (1990). Isoprenylation is required for the processing of the lamin A precursor. *Journal of Cell Biology, 110*(5), 1489-1499.

Bernier-Villamor, V., Sampson, D. A., Matunis, M. J., & Lima, C. D. (2002). Structural basis for E2-mediated SUMO conjugation revealed by a complex between ubiquitin-conjugating enzyme Ubc9 and RanGAP1. *Cell, 108*(3), 345-356.

Black, D. L. (2003). *Mechanisms of alternative pre-messenger RNA splicing*

Bohren, K. M., Nadkarni, V., Song, J. H., Gabbay, K. H., & Owerbach, D. (2004). A M55V polymorphism in a novel SUMO gene (SUMO-4) differentially activates heat shock transcription factors and is associated with susceptibility to type I diabetes mellitus.

Journal of Biological Chemistry, 279(26), 27233-27238.

Bond, U., & Schlesinger, M. J. (1985). Ubiquitin is a heat shock protein in chicken embryo fibroblasts. *Molecular and Cellular Biology, 5*(5), 949-956.

Bonne, G., Mercuri, E., Muchir, A., Urtizberea, A., Bécane, H. M., Recan, D., et al. (2000). Clinical and molecular genetic spectrum of autosomal dominant emery-dreifuss muscular dystrophy due to mutations of the lamin A/C gene. *Annals of Neurology, 48*(2), 170-180.

Braschi, E., Zunino, R., & McBride, H. M. (2009). MAPL is a new mitochondrial SUMO E3 ligase that regulates mitochondrial fission. *EMBO Reports, 10*(7), 748-754.

Burke, B., & Stewart, C. L. (2002). Life at the edge: The nuclear envelope and human disease. *Nature Reviews Molecular Cell Biology, 3*(8), 575-585.

Cartegni, L., Chew, S. L., & Krainer, A. R. (2002). Listening to silence and understanding nonsense: Exonic mutations that affect splicing. *Nature Reviews Genetics, 3*(4), 285-298.

Chabot, B. (1996). Directing alternative splicing: Cast and scenarios. *Trends in Genetics, 12*(11), 472-478.

Chatterjee, S., & Pal, J. K. (2009). Role of 5′- and 3′-untranslated regions of mRNAs in human diseases. *Biology of the Cell, 101*(5), 251-262.

Clarke, S. (1992). Protein isoprenylation and methylation at carboxyl-terminal cysteine residues. *Annual Review of Biochemistry, 61*, 355-386.

Claycomb, W. C., Lanson Jr., N. A., Stallworth, B. S., Egeland, D. B., Delcarpio, J. B., Bahinski, A., et al. (1998). HL-1 cells: A cardiac muscle cell line that contracts and retains phenotypic characteristics of the adult cardiomyocyte. *Proceedings of the National Academy of Sciences of the United States of America, 95*(6), 2979-2984.

Colgan, D. F., & Manley, J. L. (1997). Mechanism and regulation of mRNA polyadenylation. *Genes and Development, 11*(21), 2755-2766.

Constantinescu, D., Gray, H. L., Sammak, P. J., Schatten, G. P., & Csoka, A. B. (2006). Lamin A/C expression is a marker of mouse and human embryonic stem cell differentiation. *Stem Cells, 24*(1), 177-185.

Das, R., Dufu, K., Romney, B., Feldt, M., Elenko, M., & Reed, R. (2006). Functional coupling of RNAP II transcription to spliceosome assembly. *Genes and Development, 20*(9), 1100-1109.

De Sandre-Giovannoli, A., Chaouch, M., Kozlov, S., Vallat, J. -., Tazir, M., Kassouri, N., et al. (2002). Homozygous defects in LMNA, encoding lamin A/C nuclear-envelope proteins, cause autosomal recessive axonal neuropathy in human (charcot-marie-tooth

disorder type 2) and mouse. *American Journal of Human Genetics, 70*(3), 726-736.

Desterro, J. M. P., Thomson, J., & Hay, R. T. (1997). Ubch9 conjugates SUMO but not ubiquitin. *FEBS Letters, 417*(3), 297-300.

Dou, H., Huang, C., Singh, M., Carpenter, P. B., & Yeh, E. T. H. (2010). Regulation of DNA repair through DeSUMOylation and SUMOylation of replication protein A complex. *Molecular Cell, 39*(3), 333-345.

Dreuillet, C., Tillit, J., Kress, M., & Ernoult-Lange, M. (2002). In vivo and in vitro interaction between human transcription factor MOK2 and nuclear lamin A/C. *Nucleic Acids Research, 30*(21), 4634-4642.

Emery, A. E. H. (1989). Emery-dreifuss syndrome. *Journal of Medical Genetics, 26*(10), 637-641.

Eriksson, M., Brown, W. T., Gordon, L. B., Glynn, M. W., Singer, J., Scott, L., et al. (2003). Recurrent de novo point mutations in lamin A cause hutchinson-gilford progeria syndrome. *Nature, 423*(6937), 293-298.

Estève, P. -., Chin, H. G., Benner, J., Feehery, G. R., Samaranayake, M., Horwitz, G. A., et al. (2009). Regulation of DNMT1 stability through SET7-mediated lysine methylation in mammalian cells. *Proceedings of the National Academy of Sciences of the United States of America, 106*(13), 5076-5081.

Fatkin, D., Macrae, C., Sasaki, T., Wolff, M. R., Porcu, M., Frenneaux, M., et al. (1999). Missense mutations in the rod domain of the lamin A/C gene as causes of dilated cardiomyopathy and conduction-system disease. *New England Journal of Medicine, 341*(23), 1715-1724.

Favreau, C., Higuet, D., Courvalin, J. -., & Buendia, B. (2004). Expression of a mutant lamin A that causes emery-dreifuss muscular dystrophy inhibits in vitro differentiation of C2C12 myoblasts. *Molecular and Cellular Biology, 24*(4), 1481-1492.

Flanagan, J. F., Mi, L., Chruszcz, M., Cymborowski, M., Clines, K. L., Kim, Y., et al. (2005). Double chromodomains cooperate to recognize the methylated histone H3 tail. *Nature, 438*(7071), 1181-1185.

Garg, A. (2000). Lipodystrophies. *American Journal of Medicine, 108*(2), 143-152.

Geiss-Friedlander, R., & Melchior, F. (2007). Concepts in sumoylation: A decade on. *Nature Reviews Molecular Cell Biology, 8*(12), 947-956.

Genschel, J., & Schmidt, H. H. -. (2000). Mutations in the LMNA gene encoding lamin A/C. *Human Mutation, 16*(6), 451-459.

Gerace, L., & Blobel, G. (1980). The nuclear envelope lamina is reversibly depolymerized during mitosis. *Cell, 19*(1), 277-287.

Gershey, E. L., Vidali, G., & Allfrey, V. G. (1968). Chemical studies of histone acetylation. the occurrence of epsilon-N-acetyllysine in the f2a1 histone. *Journal of Biological Chemistry, 243*(19), 5018-5022.

Glotzer, M., Murray, A. W., & Kirschner, M. W. (1991). Cyclin is degraded by the ubiquitin pathway. *Nature, 349*(6305), 132-138.

Gray, N. K., & Wickens, M. (1998). *Control of translation initiation in animals*

Hay, R. T. (2005). SUMO: A history of modification. *Molecular Cell, 18*(1), 1-12.

Hicke, L., Schubert, H. L., & Hill, C. P. (2005). Ubiquitin-binding domains. *Nature Reviews Molecular Cell Biology, 6*(8), 610-621.

Hübner, S., Eam, J. E., Hübner, A., & Jans, D. A. (2006). Laminopathy-inducing lamin A mutants can induce redistribution of lamin binding proteins into nuclear aggregates. *Experimental Cell Research, 312*(2), 171-183.

Jang, S. K., Krausslich, H. -., Nicklin, M. J. H., Duke, G. M., Palmenberg, A. C., & Wimmer, E. (1988). A segment of the 5' nontranslated region of encephalomyocarditis virus RNA directs internal entry of ribosomes during in vitro translation. *Journal of Virology, 62*(8), 2636-2643.

Jenuwein, T., & Allis, C. D. (2001). Translating the histone code. *Science, 293*(5532), 1074-1080.

Johnson, E. S. (2004). *Protein modification by SUMO*

Johnson, E. S., Schwienhorst, I., Dohmen, R. J., & Blobel, G. (1997). The ubiquitin-like protein Smt3p is activated for conjugation to other proteins by an Aos1p/Uba2p heterodimer. *EMBO Journal, 16*(18), 5509-5519.

Jürgen Dohmen, R. (2004). SUMO protein modification. *Biochimica Et Biophysica Acta - Molecular Cell Research, 1695*(1-3), 113-131.

Kachirskaia, I., Shi, X., Yamaguchi, H., Tanoue, K., Wen, H., Wang, E. W., et al. (2008). Role for 53BP1 tudor domain recognition of p53 dimethylated at lysine 382 in DNA damage signaling. *Journal of Biological Chemistry, 283*(50), 34660-34666.

Kakimoto, Y. (1971). Methylation of arginine and lysine residues of cerebral proteins. *BBA - Protein Structure, 243*(1), 31-37.

Kawakami, T., Chiba, T., Suzuki, T., Iwai, K., Yamanaka, K., Minato, N., et al. (2001). NEDD8 recruits E2-ubiquitin to SCF E3 ligase. *EMBO Journal, 20*(15), 4003-4012.

Kim, E., Goren, A., & Ast, G. (2008). Alternative splicing: Current perspectives. *BioEssays, 30*(1), 38-47.

Kim, E., Magen, A., & Ast, G. (2007). Different levels of alternative splicing among eukaryotes. *Nucleic Acids Research, 35*(1), 125-131.

Krämer, A. (1996). *The structure and function of proteins involved in mammalian pre-mRNA splicing*

Krohne, G., & Benavente, R. (1986). The nuclear lamins. A multigene family of proteins in evolution and differentiation. *Experimental Cell Research, 162*(1), 1-10.

Kumar, S., Yoshida, Y., & Noda, M. (1993). Cloning of a cDNA which encodes a novel ubiquitin-like protein. *Biochemical and Biophysical Research Communications, 195*(1), 393-399.

Lander, E. S., Linton, L. M., Birren, B., Nusbaum, C., Zody, M. C., Baldwin, J., et al. (2001). Initial sequencing and analysis of the human genome. *Nature, 409*(6822), 860-921.

Lim, L. P., & Burge, C. B. (2001). A computational analysis of sequence features involved in recognition of short introns. *Proceedings of the National Academy of Sciences of the United States of America, 98*(20), 11193-11198.

Lin, F., & Worman, H. J. (1993). Structural organization of the human gene encoding nuclear lamin A and nuclear lamin C. *Journal of Biological Chemistry, 268*(22), 16321-16326.

Macejak, D. G., & Sarnow, P. (1991). Internal initiation of translation mediated by the 5' leader of a cellular mRNA. *Nature, 353*(6339), 90-94.

Machiels, B. M., Zorenc, A. H. G., Endert, J. M., Kuijpers, H. J. H., Van Eys, G. J. J. M., Ramaekers, F. C. S., et al. (1996). An alternative splicing product of the lamin A/C gene lacks exon 10. *Journal of Biological Chemistry, 271*(16), 9249-9253.

Mahajan, R., Gerace, L., & Melchior, F. (1998). Molecular characterization of the SUMO-1 modification of RanGAP1 and its role in nuclear envelope association. *Journal of Cell Biology, 140*(2), 259-270.

Matunis, M. J., Coutavas, E., & Blobel, G. (1996). A novel ubiquitin-like modification modulates the partitioning of the ran-GTPase-activating protein RanGAP1 between the cytosol and the nuclear pore complex. *Journal of Cell Biology, 135*(6), 1457-1470.

Meek, D. W. (1994). Post-translational modification of p53. *Seminars in Cancer Biology, 5*(3), 203-210.

Meluh, P. B., & Koshland, D. (1995). Evidence that the MIF2 gene of saccharomyces cerevisiae encodes a centromere protein with homology to the mammalian centromere protein CENP-C. *Molecular Biology of the Cell, 6*(7), 793-807.

Moir, R. D., Spann, T. P., Herrmann, H., & Goldman, R. D. (2000). Disruption of nuclear

lamin organization blocks the elongation phase of DNA replication. *Journal of Cell Biology, 149*(6), 1179-1191.

Mokrejš, M., Mašek, T., Vopálenský, V., Hlubuček, P., Delbos, P., & Pospíšek, M. (2009). IRESite A tool for the examination of viral and cellular internal ribosome entry sites. *Nucleic Acids Research, 38*(SUPPL.1), D131-D136.

Molkentin, J. D., Lin, Q., Duncan, S. A., & Olson, E. N. (1997). Requirement of the transcription factor GATA4 for heart tube formation and ventral morphogenesis. *Genes and Development, 11*(8), 1061-1072.

Mullen, J. R., & Brill, S. J. (2008). Activation of the Slx5-Slx8 ubiquitin ligase by poly-small ubiquitin-like modifier conjugates. *Journal of Biological Chemistry, 283*(29), 19912-19921.

Navarro, C. L., De Sandre-Giovannoli, A., Bernard, R., Boccaccio, I., Boyer, A., Geneviève, D., et al. (2004). Lamin A and ZMPSTE24 (FACE-1) defects cause nuclear disorganization and identify restrictive dermopathy as a lethal neonatal laminopathy. *Human Molecular Genetics, 13*(20), 2493-2503.

Palombella, V. J., Rando, O. J., Goldberg, A. L., & Maniatis, T. (1994). The ubiquitin-proteasome pathway is required for processing the NF-κB1 precursor protein and the activation of NF-κB. *Cell, 78*(5), 773-785.

Pelletier, J., & Sonenberg, N. (1988). Internal initiation of translation of eukaryotic mRNA directed by a sequence derived from poliovirus RNA. *Nature, 334*(6180), 320-325.

Pickering, B. M., & Willis, A. E. (2005). The implications of structured 5′ untranslated regions on translation and disease. *Seminars in Cell and Developmental Biology, 16*(1), 39-47.

Pu, W. T., Ishiwata, T., Juraszek, A. L., Ma, Q., & Izumo, S. (2004). GATA4 is a dosage-sensitive regulator of cardiac morphogenesis. *Developmental Biology, 275*(1), 235-244.

Reamon-Buettner, S., Cho, S. -., & Borlak, J. (2007). Mutations in the 3′-untranslated region of GATA4 as molecular hotspots for congenital heart disease (CHD). *BMC Medical Genetics, 8*

Rino, J., & Carmo-Fonseca, M. (2009). The spliceosome: A self-organized macromolecular machine in the nucleus? *Trends in Cell Biology, 19*(8), 375-384.

Ritchie, D. B., Schellenberg, M. J., & MacMillan, A. M. (2009). Spliceosome structure: Piece by piece. *Biochimica Et Biophysica Acta - Gene Regulatory Mechanisms, 1789*(9-10), 624-633.

Rober, R. -., Weber, K., & Osborn, M. (1989). Differential timing of nuclear lamin A/C expression in the various organs of the mouse embryo and the young animal: A

developmental study. *Development, 105*(2), 365-378.

Robins, M. J., MacCoss, M., & Lee, A. S. K. (1976). Nucleic acid related compounds. 20. sugar, base doubly modified nucleosides at the 5' terminal 'cap' of mRNAs and in nuclear RNA. *Biochemical and Biophysical Research Communications, 70*(2), 356-363.

Roy, S. W., & Irimia, M. (2009). Splicing in the eukaryotic ancestor: Form, function and dysfunction. *Trends in Ecology and Evolution, 24*(8), 447-455.

Saitoh, H., & Hinchey, J. (2000). Functional heterogeneity of small ubiquitin-related protein modifiers SUMO-1 versus SUMO-2/3. *Journal of Biological Chemistry, 275*(9), 6252-6258.

Sampson, D. A., Wang, M., & Matunis, M. J. (2001). The small ubiquitin-like modifier-1 (SUMO-1) consensus sequence mediates Ubc9 binding and is essential for SUMO-1 modification. *Journal of Biological Chemistry, 276*(24), 21664-21669.

Schulze, W. X. (2010). Proteomics approaches to understand protein phosphorylation in pathway modulation. *Current Opinion in Plant Biology, 13*(3), 280-287.

Schwarz, S. E., Matuschewski, K., Liakopoulos, D., Scheffner, M., & Jentsch, S. (1998). The ubiquitin-like proteins SMT3 and SUMO-1 are conjugated by the UBC9 E2 enzyme. *Proceedings of the National Academy of Sciences of the United States of America, 95*(2), 560-564.

Sinensky, M., Fantle, K., Trujillo, M., McLain, T., Kupfer, A., & Dalton, M. (1994). The processing pathway of prelamin A. *Journal of Cell Science, 107*(1), 61-67.

Speckman, R. A., Garg, A., Du, F., Bennett, L., Veile, R., Arioglu, E., et al. (2000). Mutational and haplotype analyses of families with familial partial lipodystrophy (dunnigan variety) reveal recurrent missense mutations in the global C-terminal domain of lamin A/C. *American Journal of Human Genetics, 66*(4), 1192-1198.

Stuurman, N., Heins, S., & Aebi, U. (1998). Nuclear lamins: Their structure, assembly, and interactions. *Journal of Structural Biology, 122*(1-2), 42-66.

Sugnet, C. W., Kent, W. J., Ares Jr., M., & Haussler, D. (2004). Transcriptome and genome conservation of alternative splicing events in humans and mice. *Pacific Symposium on Biocomputing.Pacific Symposium on Biocomputing,* , 66-77.

Tatham, M. H., Jaffray, E., Vaughan, O. A., Desterro, J. M. P., Botting, C. H., Naismith, J. H., et al. (2001). Polymeric chains of SUMO-2 and SUMO-3 are conjugated to protein substrates by SAE1/SAE2 and Ubc9. *Journal of Biological Chemistry, 276*(38), 35368-35374.

Tatham, M. H., Rodriguez, M. S., Xirodimas, D. P., & Hay, R. T. (2009). Detection of protein SUMOylation in vivo. *Nature Protocols, 4*(9), 1363-1371.

Tazi, J., Bakkour, N., & Stamm, S. (2009). Alternative splicing and disease. *Biochimica Et Biophysica Acta - Molecular Basis of Disease, 1792*(1), 14-26.

Thorne, R. F., Ralston, K. J., de Bock, C. E., Mhaidat, N. M., Zhang, X. D., Boyd, A. W., et al. (2010). Palmitoylation of CD36/FAT regulates the rate of its post-transcriptional processing in the endoplasmic reticulum. *Biochimica Et Biophysica Acta - Molecular Cell Research, 1803*(11), 1298-1307.

Thorrez, L., Van Deun, K., Tranchevent, L. -., Van Lommel, L., Engelen, K., Marchal, K., et al. (2008). Using ribosomal protein genes as reference: A tale of caution. *PLoS ONE, 3*(3)

Ulrich, H. D. (2008). The fast-growing business of SUMO chains. *Molecular Cell, 32*(3), 301-305.

Van Engelen, B. G. M., Muchir, A., Hutchison, C. J., Van Der Kooi, A. J., Bonne, G., & Lammens, M. (2005). The lethal phenotype of a homozygous nonsense mutation in the lamin A/C gene. *Neurology, 64*(2), 374-376.

Vertegaal, A. C. O., Andersen, J. S., Ogg, S. C., Hay, R. T., Mann, M., & Lamond, A. I. (2006). Distinct and overlapping sets of SUMO-1 and SUMO-2 target proteins revealed by quantitative proteomics. *Molecular and Cellular Proteomics, 5*(12), 2298-2310.

Wakamatsu, A., Kimura, K., Yamamoto, J. -., Nishikawa, T., Nomura, N., Sugano, S., et al. (2009). Identification and functional analyses of 11 769 full-length human cDNAs focused on alternative splicing. *DNA Research, 16*(6), 371-383.

Wang, E. T., Sandberg, R., Luo, S., Khrebtukova, I., Zhang, L., Mayr, C., et al. (2008). Alternative isoform regulation in human tissue transcriptomes. *Nature, 456*(7221), 470-476.

Weber, K., Plessmann, U., & Traub, P. (1989). Maturation of nuclear lamin A involves a specific carboxy-terminal trimming, which removes the polyisoprenylation site from the precursor; implications for the structure of the nuclear lamina. *FEBS Letters, 257*(2), 411-414.

Wilkinson, K. A., Nishimune, A., & Henley, J. M. (2008). Analysis of SUMO-1 modification of neuronal proteins containing consensus SUMOylation motifs. *Neuroscience Letters, 436*(2), 239-244.

Wilson, K. L. (2000). The nuclear envelope, muscular dystrophy and gene expression. *Trends in Cell Biology, 10*(4), 125-129.

Wold, F. (1981). In vivo chemical modification of proteins (post-translational modification). *Annual Review of Biochemistry, 50*, 783-814.

Worman, H. J., Fong, L. G., Muchir, A., & Young, S. G. (2009). Laminopathies and the

long strange trip from basic cell biology to therapy. *Journal of Clinical Investigation, 119*(7), 1825-1836.

Yaffe, D., & Saxel, O. (1977). Serial passaging and differentiation of myogenic cells isolated from dystrophic mouse muscle. *Nature, 270*(5639), 725-727.

Yang, S. -., Galanis, A., Witty, J., & Sharrocks, A. D. (2006). An extended consensus motif enhances the specificity of substrate modification by SUMO. *EMBO Journal, 25*(21), 5083-5093.

Zhang, H., Hu, J., Recce, M., & Tian, B. (2005). PolyA_DB: A database for mammalian mRNA polyadenylation. *Nucleic Acids Research, 33*(DATABASE ISS.), D116-D120.

Zhang, Y. -., & Sarge, K. D. (2008). Sumoylation regulates lamin A function and is lost in lamin A mutants associated with familial cardiomyopathies. Journal of Cell Biology, 182(1), 35-39.

Permission for figures

NATURE PUBLISHING GROUP LICENSE TERMS AND CONDITIONS

Apr 05, 2011

This is a License Agreement between Shelley A Deeke ("You") and Nature Publishing Group ("Nature Publishing Group") provided by Copyright Clearance Center ("CCC"). The license consists of your order details, the terms and conditions provided by Nature Publishing Group, and the payment terms and conditions.

All payments must be made in full to CCC. For payment instructions, please see information listed at the bottom of this form.

License Number	2563101232378
License date	Dec 06, 2010
Licensed content publisher	Nature Publishing Group
Licensed content publication	Nature Reviews Genetics
Licensed content title	Listening to silence and understanding nonsense: exonic mutations that affect splicing
Licensed content author	Luca Cartegni, Shern L. Chew, Adrian R. Krainer
Licensed content date	Apr 1, 2002
Type of Use	reuse in a thesis/dissertation
Requestor type	academic/educational
Format	print and electronic
Portion	figures/tables/illustrations
Number of figures/tables/illustrations	1
High-res required	no
Figures	Figure 1b: Classical splicing signals and modes of alternative splicing
Author of this NPG article	no
Your reference number	
Title of your thesis / dissertation	Identifying the isoforms of a novel Musle-enriched A-type Lamin-Interacting Protein
Expected completion date	Jan 2011
Estimated size (number of pages)	100
Total	0.00 USD

NATURE PUBLISHING GROUP LICENSE TERMS AND CONDITIONS

Apr 05, 2011

This is a License Agreement between Shelley A Deeke ("You") and Nature Publishing Group ("Nature Publishing Group") provided by Copyright Clearance Center ("CCC"). The license consists of your order details, the terms and conditions provided by Nature Publishing Group, and the payment terms and conditions.

All payments must be made in full to CCC. For payment instructions, please see information listed at the bottom of this form.

License Number	2582030805102
License date	Jan 04, 2011
Licensed content publisher	Nature Publishing Group
Licensed content publication	Nature Reviews Molecular Cell Biology
Licensed content title	Life at the edge: the nuclear envelope and human disease
Licensed content author	Brian Burke, Colin L. Stewart
Licensed content date	Aug 1, 2002
Type of Use	reuse in a thesis/dissertation
Requestor type	academic/educational
Format	print and electronic
Portion	figures/tables/illustrations
Number of figures/tables/illustrations	1
High-res required	no
Figures	Figure 4:Laminopathy-linked LMNA mutations.
Author of this NPG article	no
Your reference number	
Title of your thesis / dissertation	Identifying the isoforms of a novel Musle-enriched A-type Lamin-Interacting Protein
Expected completion date	Jan 2011
Estimated size (number of pages)	100
Total	0.00 USD

NATURE PUBLISHING GROUP LICENSE
TERMS AND CONDITIONS

Apr 05, 2011

This is a License Agreement between Shelley A Deeke ("You") and Nature Publishing Group ("Nature Publishing Group") provided by Copyright Clearance Center ("CCC"). The license consists of your order details, the terms and conditions provided by Nature Publishing Group, and the payment terms and conditions.

All payments must be made in full to CCC. For payment instructions, please see information listed at the bottom of this form.

License Number	2558220436930
License date	Nov 29, 2010
Licensed content publisher	Nature Publishing Group
Licensed content publication	Nature Reviews Molecular Cell Biology
Licensed content title	Concepts in sumoylation: a decade on
Licensed content author	Ruth Geiss-Friedlander, Frauke Melchior
Licensed content date	Dec 1, 2007
Type of Use	Thesis / Dissertation
Pages	
Portion used	Figures / tables
Number of figures / tables	1
Requestor type	Student
Details of use	STM signatory
Total	0.00 USD
Terms and Conditions	

Curriculum Vitae

SHELLEY ANN DEEKE

Summary of Skills and Qualifications

- Masters of Science in Biochemistry
- Fluent in both official languages
- Software skills : Microsoft Office, Microsoft Excel, Powerpoint, WordPerfect Office,
- Problem solving, critical thinking, job task planning and organizing, continuous learning.

Education

M.Sc. candidate Biochemistry **Present**
Identifying the isoforms of a novel Musle-enriched A-type Lamin-Interacting Protein
University of Ottawa Heart Institute, Faculty of Medicine, Ontario

Bachelor of Science, Honours in Biochemistry **2008**
University of Ottawa, Ontario

WHMIS, Animal Care, Health and Safety **2008**
University of Ottawa, Ontario

Awards

Biochemistry Travel Award	**2009**
Graduate studies admission scholarship, University of Ottawa	**2008-2010**
Laboratory Rotation for Summer Graduate Students BCH Graduate Program	**2008**
Graduated cum laude from University	**2008**
Deans list, University of Ottawa	**2007-2008**
Fellowship for Studying in French scholarship	**2004-2005**
Admission scholarship University of Ottawa	**2004**
Award for highest average in biology, École Secondaire Embrun	**2004**

Relevant Skills

- Knowledge of laboratory equipment, procedures and data analysis for biochemistry and molecular biology: cell culture techniques; isolating and purifying RNA and protein from animal tissues and cells; cloning and sequencing; Western blotting; RT-PCR; DNA electrophoresis; Immunohistochemistry; Two-dimensional electrophoresis; Transfections; Immunoprecipitations; Site-Directed Mutagenesis; Isolation and purification of recombinant proteins; *in vitro* SUMOylation assay; 5' and 3' rapid amplification of complementary DNA ends
- Comfortable with bioinformatic sites: PubMed, Scopus, BLAST, NEBcutter, UCSC Genome Browser, ClustalW2.

- Preparing and delivery of presentations, analytical skills, troubleshooting and data organization

Conferences/Seminars

Poster Presentation ."Developmental and molecular bases of LTIF in cell fate determination". The Ottawa Conference on New Directions in Biology and Disease of Skeletal Muscle, Westin Hotel, Ottawa, Ontario **May 2010**

Participated in "Making Muscle in the Embryo and Adult" conference Columbia University, New York, New York **June 2009**

Publications

Teng AC, Kuraitis D, **Deeke SA**, Ahmadi A, Dugan SG, Cheng BL, Crowson MG, Burgon PG, Suuronen EJ, Chen HH, Stewart AF. IRF2BP2 is a skeletal and cardiac muscle-enriched ischemia-inducible activator of VEGFA expression. *FASEB J*. 2010 Aug 23. [Epub ahead of print]

Employment Experience

Customer Service representative **2007-Present**
Gamma-Dynacare Medical Laboratories

- Key responsibilities include: contacting clients to report STAT, critical and abnormal results, maintain confidentiality and accuracy of appropriate documentation. Answering inquiries from clients and Patient Service Centres. Solving and documenting incoming problems. Retrieval of images of requisitions and ECG's.

Special Services Associate **2006-2007**
Home Depot, Orleans, Ontario

- Key responsibilities include: ensuring that customers receive both the products they ordered and the services they requested in an accurate and timely manner. Interact with vendors, installers, associates in the store, trucking/shipping companies and the customers themselves to ensure that excellent customer service is achieved.

Swimming Instructor and Lifeguard **2003-2005**
Norm's Gym Embrun, Ontario.

- In both official languages, taught Red Cross Aqua-quest Levels 1-5, Aquatots 1-3. Lesson planning and student evaluations. Lifeguard birthday parties and summer camp. Employed part time during school year and fulltime during the summer.

Volunteer Experience

The Carleton Cup fundraiser **January 2010**
Canadian Cystic Fibrosis Foundation

- Documenting competitors finishing times
- Merchandise sales

Brain Awareness Week **March 2010**

Presentation of facts regarding the brain to elementary students

Ormond Recreational Association **1998-2004**

- Assisted coordinators in providing activities throughout the year, including preparations, provision, clean up, snacks, crafts, games and decorating

Winchester Dance Club **2000-2002**

- Assisted in providing dance instruction

Metcalfe Spark Unit **2001-2002**

- Assisted in providing snacks, games, educational activities and crafts